

Mechanism of Action of a Therapeutic Peptide,
Risuteganib, Suggests that Supporting Mitochondrial
Function Underlies its Clinical Efficacy in Treating
Leading Causes of Blindness

Thesis by
Dan Zhou

In Partial Fulfillment of the Requirements for
the Degree of
Doctor of Philosophy

The logo for the California Institute of Technology (Caltech), featuring the word "Caltech" in a bold, orange, sans-serif font.

CALIFORNIA INSTITUTE OF TECHNOLOGY
Pasadena, California

2021
(Defended on May 14, 2021)

© 2021

Dan Zhou

ORCID: 0000-0003-2367-2822

All rights reserved

ACKNOWLEDGEMENTS

First of all, thank you for reading my thesis. I appreciate the time you spend, and I hope you will enjoy reading this thesis. In the meantime, thank you for bearing with me and with my non-native English writing.

It is unbelievable when I looked back how much my studies at Caltech have changed my view of life and of the world. Caltech taught me a lot of things. The most beautiful thing is the art of science. The moment a bell rang in my head was when I came up with a hypothesis that could explain the drug efficacy in disease management. Being able to understand the science behind the research and apply the knowledge to guide the research directions is exciting and satisfying. I still feel my heartbeat quicken every time I talk about my research work. This experience also allows me to appreciate the art of science in other research fields, which really opens up my mind to the world.

The other really important thing I learnt is problem solving, which I should say came mostly from my advisor, Prof. Julie Kornfield. I am deeply influenced by how Julie sees through scientific data, digs into the value of the problems, brainstorms on solutions to solve the problems, and continues digging more into the science behind it. She has inspired me in numerous ways, on my projects that I worked on, my scientific thinking and writing, and also my work styles as I grew into a better scientist. I really enjoyed our lecture circuit trips to China, during which I got to know Julie in person as a scientist and as a friend. Although she made my life really tough sometimes, now I look at it as a good training of how to push

back and handle conflicts of opinions. I received huge support from Julie during my toughest time, and it was one of the most important reasons that I made it to today. Thank you Julie!

I would really like to thank the people who supported me during my graduate study:

To Dr. Cris Kenney and Dr. Marilyn Chwa at UC Irvine, thank you for allowing me to study mitochondrial functions in your lab. I really appreciate your support and advice during my stay. Thank you for treating me as one of your pals. It was a really pleasant experience to work with you. I also realized that not everyone works like Julie (sorry Julie ☺).

To Dr. John Park, and all other collaborators at Allegro Ophthalmics, I am grateful that you funded this project, innovated risuteganib and made it available to us, shared the research studies from different groups, and moved forward the clinical trials with incredible progress. I hope everything will go well with you and the clinical trials of risuteganib.

To Dr. Peter Campochiaro at JHMS and Dr. Douglas Vollrath at Stanford, thank you for the discussions we had in 2017 ARVO meeting. It was one of the most unforgettable moments in my life, and I deeply appreciate all the inspirations you gave me.

To Dr. Mona Shahgholi at Caltech Mass Spec Lab, thank you for being such a good friend. I really enjoyed the time we spent together to make mass spec imaging work. I love to work

with you and thank you so much for inspiring me. I will always remember the day that I talked to you and realized that I still love science.

To my lab mates, thank you: Dr. Zach Shao and Jin Mo Koo, for working with me on this project; Dr. Tiziana Di Luccio, for being like a sister to me, and taking good care of me; Dr. Amy Fu, and Dr. Boyu Li, for all the mentoring; Dr. Ben Laccetti and Dr. Rachel Ford, for accompanying me along the journey; Priya Chittur, for your encouragement; and all others, for your inspiration and help. We have and will survive together.

To Dr. Coleman, thank you for giving me help during my toughest time. You taught me how to be brave and to forgive.

To my family in China, thanks for bearing the time that we are separated and in different countries. If I had been studying and working in China during the past years, we could have enjoyed quality time together and not miss each other so much. 爸，妈，姐姐，这是这篇毕业论文里面唯一一句中文，我想和你们说谢谢你们，我爱你们! (To my Dad, Mum, and sister, in the only sentence that you would understand in this entire thesis, I want to thank you and tell you that I love you very much!)

Finally, to my beloved husband, Sanle Hu. Sorry for all the ugly sides of me that I only reveal to you. You always know how to cheer me up when I am down. I enjoyed every meal you made that allowed me to survive through graduate life. Thank you for the sacrifices and burden you took during my toughest time. I would not had made it this far without you!

ABSTRACT

Age-related macular degeneration (AMD) and diabetic retinopathy (DR) are the leading causes of blindness in the developed world and on the rise globally due to the growth of an aging population and an increasing number of diabetics. Antibodies of vascular endothelial growth factor (VEGF), which target neovascularization in the advanced stages of both diseases, have been the main treatment for the past decade. However, anti-VEGF therapies suffer from short half-life and high cost inherent to antibodies, limiting the medical availability to a broader population.

To fill the unmet medical need for treating retinal diseases, a novel therapeutic oligopeptide, risuteganib, is currently in Phase II clinical trials. Results from completed trials suggest that risuteganib has comparable drug efficacy to anti-VEGF therapies, long half-life, low cost, and absence of drug-related adverse events in several hundred patients enrolled in clinical trials for diabetic macular edema (DME) and dry AMD. Risuteganib was originally designed to target neovascularization, intending to inhibit integrin cell-surface receptors and thereby block adhesion and migration of abnormal blood vessel cells. Early in our study, we found experimental evidence contrary to this mechanism of action (MOA).

Our journey began with an unbiased search for the binding loci in retinal tissue, using peptide-directed fluorescent labeling. We found out that risuteganib specifically binds to a monolayer of cells, the retinal pigment epithelium (RPE), which has essential functions in maintaining the homeostasis of the retina, and its dysfunction is the hallmark for both

blinding retinal diseases. *In vitro* study in an RPE cell model, ARPE19, showed that risuteganib protects cells against elevated oxidative stress that is associated with AMD and DR. This protective effect correlates with maintaining mitochondrial function. Further study of mitochondrial bioenergetics, in collaboration with Dr. Cris Kenney at UCI, revealed that risuteganib supports oxidative phosphorylation metabolism in the mitochondria.

Based on the chemical similarity of risuteganib with a natural product, we hypothesized that risuteganib may act through a mitochondrial enzyme, pyruvate dehydrogenase kinase (PDK), specifically PDK1 that is responsive to disease-related hypoxia-inducible factor 1 alpha (HIF-1 α). Protein phosphorylation assay and enzymatic assay confirmed that risuteganib inhibits PDK1, as a result, reducing phosphorylation of an essential enzyme, pyruvate dehydrogenase (PDH). Leaving PDH in its unphosphorylated form allows its continued activity in oxidative phosphorylation metabolism, which offers a molecular explanation of the ability to support mitochondrial activity. This leads to our current hypothesis that risuteganib's mechanism of action (MOA) is through inhibition of PDK and protection of mitochondrial functions in RPE cells for treating retinal diseases.

Protecting mitochondrial functions may be beneficial to other cell types and in other diseases that subject cells to oxidative stress. As the mitochondria targeting is a potential therapy for diverse life-threatening diseases, including inflammatory disease, cardiovascular disease, and cancer, the present hypothesis invites us to expand our scope of view for this study to broader applications.

PUBLISHED CONTENT AND CONTRIBUTIONS

Zhou, Dan et al. (2020) Mechanism of Action of Risuteganib for Retinal Diseases through Protection of Retinal Pigment Epithelium (RPE) and Enhancement of Mitochondrial Functions. *Investigative Ophthalmology and Visual Science*, 61 (7). Art. No. 4949. ISSN 0146-0404. URL: <https://iovs.arvojournals.org/article.aspx?articleid=2768773>

- Dan Zhou was the main contributor to the conception of the project and data collection of ARPE19 cell study and mitochondrial function assays.

Zhou, Dan et al. (2017) Exploring the Mechanism of Action of a Newly-Discovered Therapeutic Peptide for Blinding Retinal Diseases by Identifying Its Receptors. In: 253rd American Chemical Society National Meeting & Exposition, April 2-6, 2017, San Francisco, CA.

- Dan Zhou was the main contributor to the conception of the project and data collection of biochemical assays in fluorescent labeling and receptor capture.

TABLE OF CONTENTS

Acknowledgements	iii
Abstract	vi
Published Content and Contributions	viii
Table of Contents	ix
List of Figures and Tables	xi
Chapter I: Introduction to retinal diseases and risuteganib	1
1.1 Leading causes of blindness.....	1
1.2 Vascular endothelial growth factor (VEGF) and current therapeutics.....	5
1.3 Risuteganib design principle and clinical observations.....	6
1.4 Integrin-binding mechanism of action overturned	11
1.5 A journey of a thousand miles begins with a single step	15
Chapter II: Finding binding loci in the retina	16
2.1 Approach to find the binding loci	16
2.2 Synthesis of peptide-fluorophore conjugate	17
2.3 Peptide-directed fluorescent staining in retinal tissue	21
2.4 ARPE19 as a cell model for retinal pigment epithelium (RPE)	29
2.5 Risuteganib protects ARPE19 cells against oxidative stress	35
2.6 Potential connection with RPE dysfunction in retinal disease.....	42
Chapter III: Risuteganib protects mitochondria through regulation of oxidative phosphorylation metabolism	43
3.1 Energetic requirements of the retina pigment epithelium (RPE)	43
3.2 Drug effect on mitochondrial respiration in RPE cells	44
3.3 Potential inhibition of pyruvate dehydrogenase kinase.....	54
3.4 Enzymatic effect in RPE cell model.....	60

3.5 Current hypothesis on mechanism of action of risuteganib	66
Chapter IV: Summary and future work	70
4.1 Retracing our path along this journey	70
4.2 Research and clinical observations agree with the current hypothesis	71
4.3 Broader context of inhibitors of pyruvate dehydrogenase kinase	73
4.4 Recommendation for future work.....	74
Appendix: Supplementary information	76
References	80

LIST OF FIGURES AND TABLES

Chapter I

Figure 1.1 Anatomy of the eye (A), the macula (B), and the disease of retinal neovascularization (C)	4
Figure 1.2 Molecular structures of RGD motif, and Risuteganib peptide	7
Figure 1.3 DME Phase II study of risuteganib showed promising drug efficacy and long-term durability.....	9
Figure 1.3 Scheme for competitive surface plasmon resonance (SPR) to measure the binding between Risuteganib and different integrin receptors.....	13
Table 1.1 Binding constant of risuteganib and RGD motif to different integrin receptors.	14

Chapter II

Figure 2.1 Molecular structures of risutagnib-Cy5 and control GRGETP-Cy5	19
Figure 2.2 Layers of the retina	22
Figure 2.3 Risuteganib preferentially binds to retinal pigment epithelial (RPE) layer	24
Figure 2.4 Summary of retinal pigment epithelium (RPE) functions	27
Figure 2.5 ARPE19 cells develop RPE phenotype characteristics and express RPE-specific protein markers, RPE65 and CRALBP.	31
Figure 2.6 Appropriately differentiated ARPE19 cells are specifically stained with risuteganib-Cy5	32
Figure 2.7 Risuteganib pre-treatment protects ARPE19 cells under oxidative stress	37

Chapter III

Figure 3.1 ATP production from aerobic respiration is much higher than anaerobic glycolysis in mitochondria	46
Figure 3.2 Risuteganib increases cellular oxidative phosphorylation in ARPE19 cells.....	48
Figure 3.3 No significant effect of Risuteganib on glycolysis in ARPE19 cells....	50
Figure 3.4 Dichloroacetic acid (DCA) is an inhibitor to pyruvate dehydrogenase kinase (PDK).....	55
Figure 3.5 PDHa1 detection of phosphorylation at Ser232 by immunoblotting	58
Figure 3.6 Pyruvate dehydrogenase (PDH) enzymatic functions and regulations .	62
Figure 3.7 Risuteganib increases pyruvate dehydrogenase (PDH) enzyme activity in ARPE19 cells	64
Figure 3.8 Proposed hypothesis of mechanism of action of risuteganib on regulating mitochondrial functions	69

Appendix

Figure S2.1 Purification of risuteganib-Cy5 (A) and GRGETP-Cy5 (B) conjugates using prep-HPLC, and characterization with MALDI-TOF	76
Figure S4.1 Colocalization of risuteganib and mitochondrial marker cytochrome c oxidase (COX IV) in rat retinal tissue	78

INTRODUCTION TO RETINAL DISEASES AND RISUTEGANIB

1.1 Leading causes of blindness

What motivates us most of this project is to find a novel therapy for treating leading causes of blindness. Age-related macular degeneration (AMD) is the top one cause of blindness in the developed world, and is a growing epidemic in many parts of the world (as health services are improving to provide treatment to other eye diseases, such as cataract)¹. It affects 30-50 million people worldwide, and these numbers are projected to increase rapidly over time with increasing number of the aging population^{2,3}. The early form of AMD, as dry AMD, characterized by the presence of fatty deposits called drusen in the macula, accounts for 85%-90% of all cases⁴. The advanced disease stage, as wet AMD, which accounts for 90% of the blindness related to AMD, is featured with abnormal blood vessels formation under the retina through a process called angiogenesis⁵. Fluid leakage from the abnormal blood in the macula distorts the structure of the retina, causes the central vision to deteriorate, and may result in permanent blindness⁶. Similar to wet AMD, diabetic macular edema (DME) as the leading cause of diabetes blindness features the hallmark of neovascularization in the macular region^{7,8}. In 2010, over one-third of an estimated 285 million people worldwide with diabetes had signs of diabetic retinopathy (DR) , and a third of these were afflicted with vision-threatening DME³.

Both of the blinding eye diseases, AMD and DME, affect the function of a fine structure in the retina, the macular region. The retina is a light-sensitive layer of tissue lining the inner surface of the eye (**Figure 1.1A**). The outermost layer, pigmented epithelium, lies on blood vessel enriched choroid which supplies the retina with oxygen and nutrients, while the innermost layer, internal limiting membrane, is attached to the gelatinous vitreous humor⁹. Near the center of the retina, there is an oval yellow spot, the macula, which contains a high density of photoreceptors and is responsible for central, high-resolution vision^{10,11} (**Figure 1.1B**). Unlike the rest of the retina, which is covered with veins and arteries as well as layers of nerve cell bodies, the macula has no blood vessels over the photoreceptors, which is essential to avoid the distortion and attenuation of light incident¹². However, restricted blood supply to the macula makes this part of the retina vulnerable to oxygen stress with its extremely high metabolic demand. Damage to the macula will result in severe loss of central vision, which is usually immediately obvious.

The vulnerability of the macular tissue relies on the mass transfer efficiency to and from the choroid to receive oxygen as well as nutrients, and to get rid of metabolic waste¹³. Both DME and AMD are asymptomatic in their early stages with the development of tiny, abnormal, leaky blood vessels inside the eye, and can progress to cause severe visual impairment. These advanced neovascular disease conditions are associated by progressive oxidative stress, inflammation, and hypoxia^{14,15}. The inflammatory cells and starved retinal cells begin releasing inflammatory cytokines and angiogenic growth factors, such as vascular endothelial growth factor (VEGF)^{16,17}, which stimulate choroidal angiogenesis or neovascularization (NV) with the breakdown of the blood-retina barrier¹⁸. These growing

blood vessels are abnormally leaky, which allows fluid to seep into the layers of macula and finally lead to pulling forces that disturb the normal structure of the eye¹⁹ (**Figure 1.1C**).

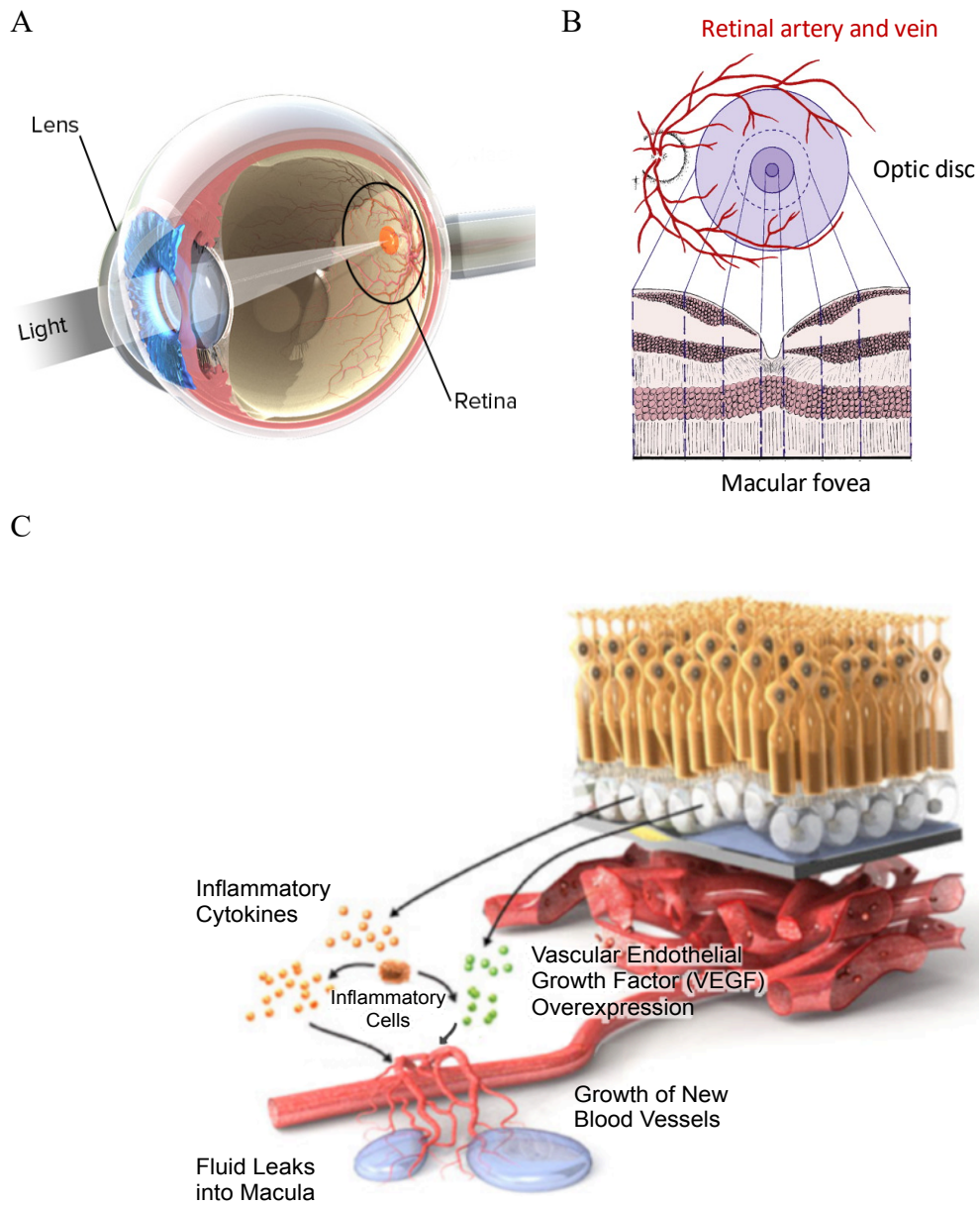


Figure 1.1. Anatomy of the eye (A), the macula (B), and the disease of retinal neovascularization (C).

1.2 Vascular endothelial growth factor (VEGF) and current therapeutics

As VEGF is one of the most important angiogenic factors released in both wet AMD and DME, pharmaceuticals based on suppression VEGF have substantially changed the management of the diseases in the past decade⁶. In 2006, landmark clinical trials showed that monthly intravitreal injections of ranibizumab (Lucentis, Genentech/Novartis) prevented vision loss in nearly 95% of patients, and significantly improved vision in 40%²⁰. Bevacizumab (Avastin, Genentech), originally developed for systemic treatment of colon cancer and related to the parent ranibizumab molecule, is now widely used as an off-label alternative²¹. In 2011, aflibercept (Eylea, Regeneron) was approved as a recombinant fusion protein with VEGF binding portions and Fc protein²². In 2019, brolocizumab (Beovu, Novartis) was approved with three-month dosing intervals²³, which added to the total five FDA approved anti-VEGF drugs for treating neovascular retinopathy.

Although anti-VEGF therapy is currently the most popular treatment for neovascularization in retinal diseases, its shortcomings of high cost and short half-life due to the nature of biologics prevent the availability to a broader population of patients²⁴. Moreover, studies show that patients with long-term drug use have a higher risk of developing advanced stage dry AMD, geographic atrophy²⁵, which is an irreversible progression of vision loss. There has been no treatment available to non-neovascular AMD, which covers a much larger patient population. The downside of anti-VEGF therapy and unmet medical needs to treat blinding diseases continue to drive the development of new therapies and pharmaceuticals.

1.3 Risuteganib design principle and clinical observations

To fill the unmet medical needs to treat the leading causes of blindness, researchers at Allegro Ophthalmics, LLC developed a hexapeptide, risuteganib (Luminate as trademark)²⁶, intended to inhibit angiogenesis through a different pathway than anti-VEGF therapy^{27,28}. Risuteganib is designed to inhibit cellular membrane protein, integrins, which are associated with cell adhesion and migration. Several proteins in this family, integrin $\alpha_v\beta_3$, $\alpha_v\beta_5$ ²⁹, and $\alpha_5\beta_1$ ³⁰ are reported to play an important role to mediate angiogenesis in the neovascular retinal diseases. Anti-integrin therapy has shown the potential to reduce the progression of the abnormal blood vessel formation with pre-clinical research and clinical trials³¹.

The chemical structure of risuteganib mimics an integrin-binding motif, Arginine-Glycine-Aspartate (RGD) sequence (**Figure 1.2**). RGD-motif was identified as the amino acid sequence in several extracellular matrix proteins, fibronectin³², vitronectin³³, and laminin³⁴, as the binding site to integrin proteins. Aspartic acid in RGD-motif is substituted with a non-canonical amino acid, Cysteic acid. As a synthetic RGD class peptide, risuteganib is intended to bind to multiple integrins, including $\alpha_v\beta_3$, $\alpha_v\beta_5$, and $\alpha_5\beta_1$, for anti-angiogenesis. Preclinical studies in choroidal neovascularization (CNV) mouse model and retinopathy of prematurity (ROP) mouse model in Dr. Peter Campochiaro's group at Wilmer Eye Institute of John Hopkins showed significant reduction of neovascularization with risuteganib treatment compared to vehicle (unpublished data).

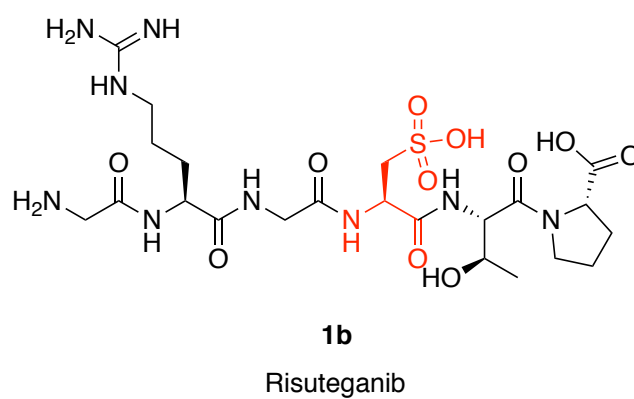
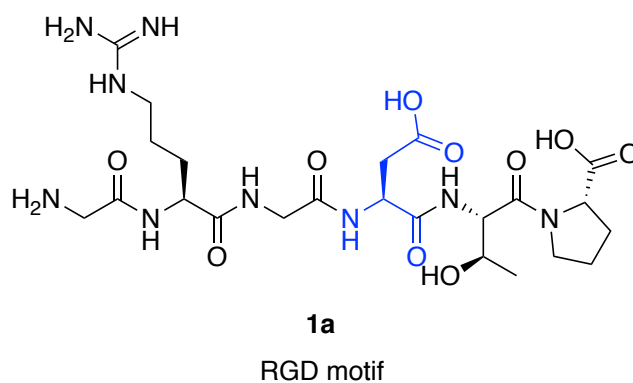
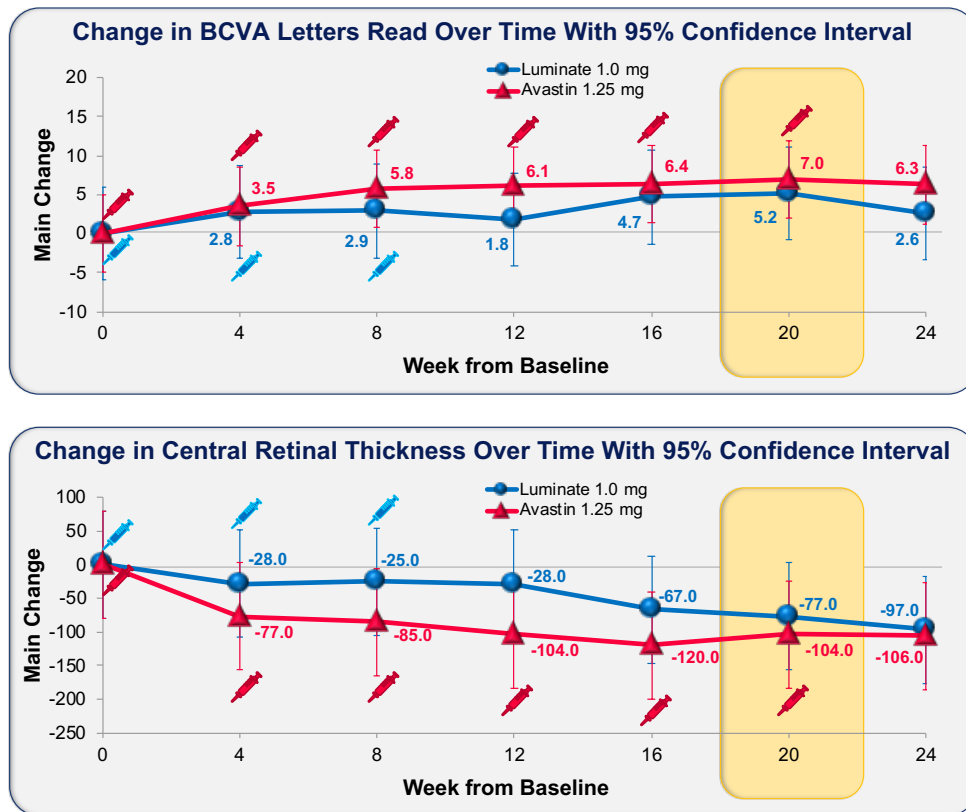


Figure 1.2 Molecular structures of RGD motif and Risuteganib peptide. These two oligopeptides share a similar sequence of 6 amino acids, glycine-arginine-glycine-X-threonine-proline (GRGXTP), while X is aspartic acid for RGD motif (**1a**) or cysteic acid for risuteganib (**1b**), labeled with different colors.

Since then, risuteganib entered clinical trials for treating DME and AMD. It has advanced through Phase I and Phase II with a total enrollment of several hundred patient subjects for safety evaluation, dose-ranging, and drug efficacy, with comparison to anti-VEGF therapy³⁵. The clinical studies demonstrated promising visual acuity gains and reduction in central macular thickness (**Figure 1.3A**) that were non-inferior to bevacizumab monotherapy. Intravitreal risuteganib was well-tolerated with no drug toxicity or intraocular inflammation and showed 12-week durability after the completion of three loading doses³⁶.

While the molecular weight of risuteganib is less than 1.0 kDa, pharmacokinetic studies showed an extraordinarily long half-life of risuteganib in the rabbit retina at 21 days (unpublished data), consistent with the 12-week durability after the completion of the initial drug doses³⁷. Optical coherence tomography (OCT) images showed that some of the study subjects produce sub-normal ending macular thicknesses consistent with the long-standing nature of their disease and the accompanying atrophy of the underlying retina (Figure 1.3B). Currently, risuteganib is planned to enter Phase III clinical trials.

A



B

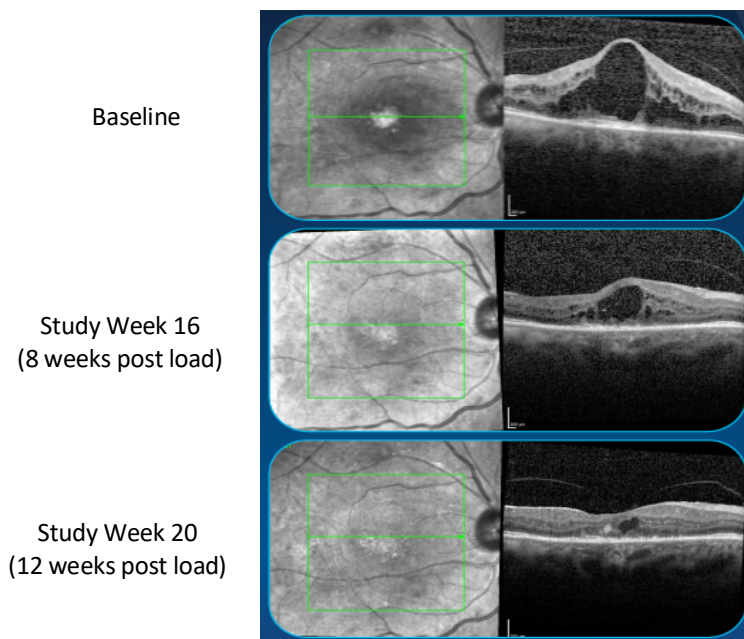


Figure 1.3 DME Phase II study of risuteganib showed promising drug efficacy and long-term durability. Risuteganib (Luminate as trademark) was administered with 3 monthly loading intravitreal injections followed by 12 weeks off treatment, compared to 6 monthly anti-VEGF bevacizumab (Avastin as trademark) injections. (A) Risuteganib is non-inferior to bevacizumab in improvement of vision acuity and reduction of central macular thickness. (B) In one patient's case that showed most vision improvement with risuteganib treatment, fluid in the macular edema was removed, and retinal thickness was significantly reduced to a sub-normal condition 12 weeks post load, measured by optical coherence tomography (OPT). BCVA: best corrected visual acuity.

1.4 Integrin-binding mechanism of action overturned

The first project in collaboration between the Kornfield group and Allegro Ophthalmics is a structure-activity relationship (SAR) study with the objectives to design and synthesize risuteganib-mimic molecules as drug candidates with enhanced efficacy. In order to compare the performance between risuteganib and its mimics, our former group member, Dr. Boyu Li, started off by measuring risuteganib binding affinity to integrin proteins, using surface plasmon resonance (SPR) technique. As binding with such a small molecule would not induce strong enough signal in SPR, a competitive assay³⁸, instead of direct binding assay between risuteganib and integrin, was designed by immobilizing integrin ligand, extracellular matrix (ECM) protein³⁹ on the SPR chip surface, followed by competitive binding between risuteganib in the flow and ECM on the surface, to integrin in the flow. The binding signal is a result of reduction in integrin binding to ECM on the surface as risuteganib concentration increases, revealing the binding affinity of risuteganib to the integrin (**Figure 1.4**). Control study was performed with RGD motif competitive assay in the same setting.

To our surprise, the binding constant of risuteganib to integrin measured in SPR study was much higher than RGD motif to integrin $\alpha_v\beta_3$, $\alpha_v\beta_5$, or $\alpha_5\beta_1$ (over 10^5 -fold, **Table 1.1**), in other words, risuteganib has very low binding affinity to integrin. Another equivalent study from our collaborator, Senju Pharmaceutical, using competitive enzyme-linked immunosorbent assay (ELISA) confirmed that the molecular binding affinity was low for risuteganib to integrin $\alpha_v\beta_3$, $\alpha_v\beta_5$, and $\alpha_{IIb}\beta_3$. They further evaluated the inhibition of the peptides to cell migration and cell proliferation, using human retinal microvascular endothelial cells, which showed that RGD motif is 100x more potent in inhibition than

risuteganib (unpublished data). The experimental evidence of molecular interactions and cell function regulations from two different research groups overturned the originally proposed mechanism of action on integrin-binding. This study became more challenging but also more exciting to uncover the MOA of risuteganib.

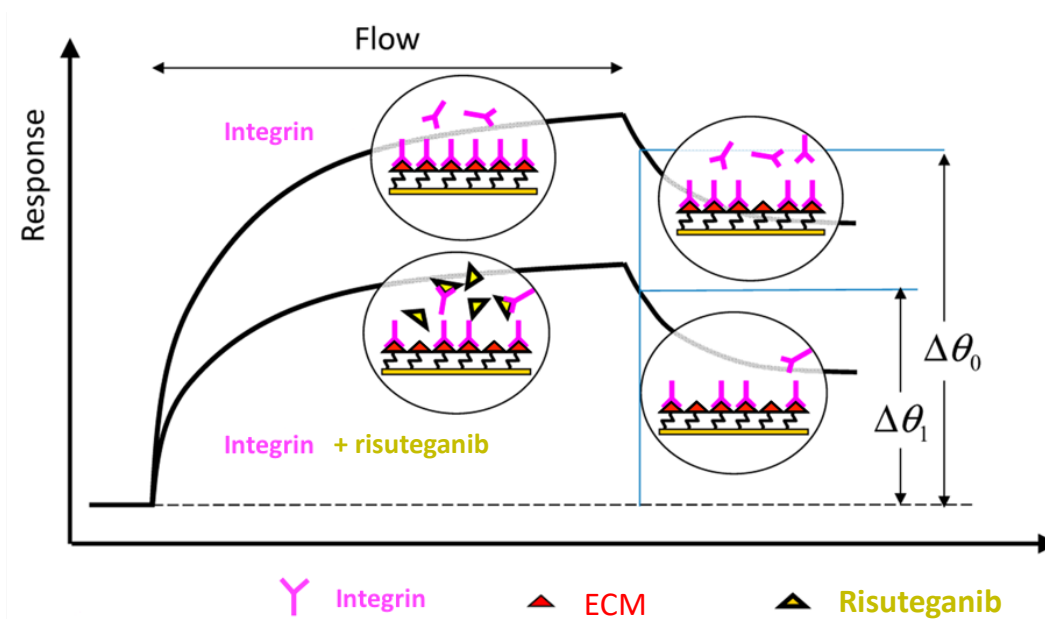


Figure 1.4 Scheme for competitive surface plasmon resonance (SPR) to measure the binding between Risuteganib and different integrin receptors. Competitive binding between Risuteganib and integrin ligands, extracellular matrix (ECM) proteins was measured.

Table1.1. Binding constant of risuteganib and RGD motif to different integrin receptors.

Integrin	ECM	Binding constant Kd (nM)	
		Risuteganib	RGD motif
$\alpha 5\beta 1$	Fibronectin	2.01×10^6	10.9
$\alpha v\beta 3$	Vitronectin	2.7×10^6	0.27
$\alpha v\beta 5$	Vitronectin	$>10^7$	<500

1.5 A journey of a thousand miles begins with a single step

That is a famous Chinese proverb, quoted from Chapter 64 of the Dao De Jing ascribed to an ancient Chinese philosopher, Laozi, about 2500 years ago. That is also how I started my thesis project in 2013 in the Kornfield lab.

We decided not to be biased by the originally proposed mechanism and set our goal to study risuteganib from the tissue interactions, to cellular interactions, and then to molecular interactions. To achieve this goal, we used peptide-directed fluorescent labeling to find the binding loci in retina, evaluated the risuteganib drug efficacy in the cell model under disease conditions (Chapter 2), found a link of risuteganib to an important cellular organelle, and hypothesized a potential molecular mechanism of how risuteganib regulates the disease management (Chapter 3). The hypothesis formed through MOA study provides insights into novel therapies for both retinal diseases, and other life-threatening diseases (Chapter 4). Here, I will start to walk you through this journey, step by step.

Chapter II

FINDING BINDING LOCI IN THE RETINA

2.1 Approach to finding the binding loci

Cells of different types in a multicellular organism, like the eyes, have dramatically different biological functions and proteomic profiles⁴⁰. Cellular receptors can be highly expressed in some cell types but not in others. In the early phase of the study, we were only looking at blood vessel cells (human umbilical vein endothelial cell model to be more specific) based on the originally proposed MOA. However, if the drug molecule, risuteganib, does not act through integrin binding, we might be studying the wrong type of cells which has low or no expression of the binding partner.

We decided to reset the project, without any bias from the previous MOA. The first step we took was to find the target cell type(s) in the retina. In this study, fluorophore-conjugated peptide was used to find the binding loci. Fluorescent labeling is widely used in biomedical research, which allows researchers to investigate the molecular interactions between a ligand and its binding partner to help understand their biological functions⁴¹. Peptides, as our drug molecule risutegnib, have been labeled with fluorescent markers and used for peptide-protein interaction studies⁴².

In this chapter, I describe how fluorophore conjugated peptide was designed, synthesized, and used as a tool to visualize specific binding in retinal tissue and cells (§2.2, §2.3). The

outcome from fluorescent labeling is further validated and connected to biological functions by studying a cell line model under a clinically relevant stress condition (§2.4, §2.5).

Each section is written as a module with its own rationale, results, discussion and methods. The result of each subsection provides the rationale for the next.

2.2 Synthesis of peptide-fluorophore conjugate

To visualize the ligand-receptor binding sites in the retinal tissue, peptide-fluorophore conjugates were designed and synthesized using standard solid phase peptide synthesis (SPPS) method. Cyanine 5 (Cy5) dye was selected for conjugation for the following reasons:

- (1) It is a bright and far-red-fluorescent label with low autofluorescence in the retinal tissue.
- (2) The retina is a neuronal organism, and Cy5 is suitable for lipophilic neuronal cell tracking.
- (3) With alkyl tails (>12 carbons) appended, Cy5 does not require additional linkers to conjugate onto the peptides. To distinguish from non-specific binding and avoid artifacts from fluorophore conjugation, we synthesized a peptide that shares sequence similarity to risuteganib as control.

2.2.1 Results

Risuteganib-Cy5 conjugate was prepared by synthesizing the peptide from C-terminus to N-terminus, and then coupling the N-terminus to the Cy5 fluorescent dye (**Figure 2.1**). A control peptide (referred to as “GRGETP” based on its amino acid sequence) was also labeled

with Cy5 dye. GRGETP differs from Risuteganib by substitution of a single amino acid cysteic acid, with a different acidic residue, glutamic acid. After solid phase peptide synthesis (SPPS) of Risuteganib-Cy5 and GRGETP-Cy5 conjugates, the crude products were purified by prep-scale high-performance liquid chromatography (HPLC). Elution fractions were collected and characterized by matrix-assisted laser desorption ionization time-of-flight (MALDI-TOF) (**Figure S2.1**). Fractions with peptide-Cy5 were lyophilized, reconstituted in DMSO, and quantified by Nanodrop.

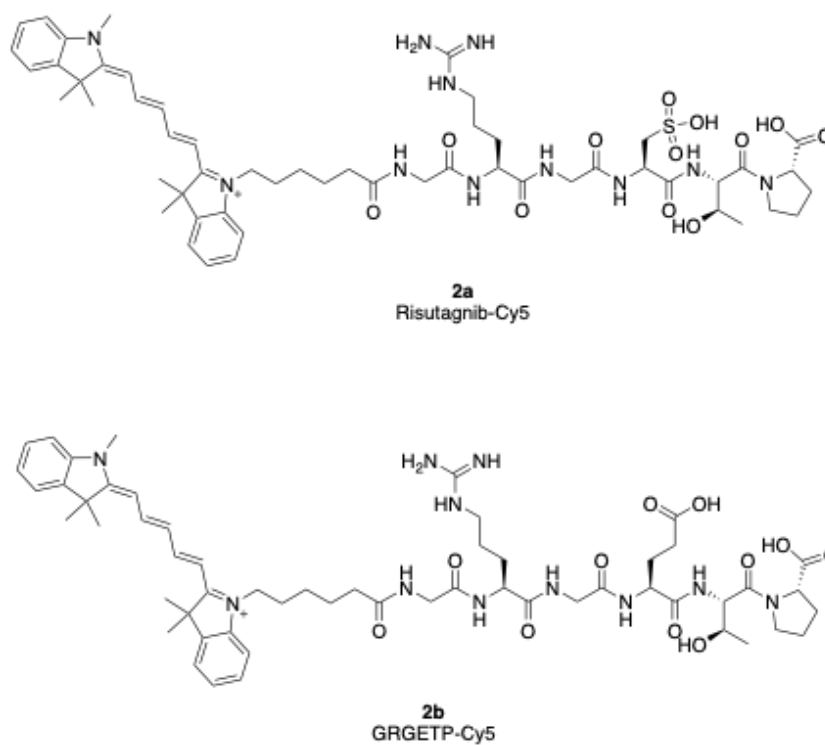


Figure 2.1 Molecular structures of risuteganib-Cy5 and control GRGETP-Cy5. Cy5 fluorescent dye was conjugated at the N-terminus for both peptides. These two molecules differ only in a single amino acid, cysteine acid (risuteganib) vs glutamic acid (GRGETP)

2.2.2 Methods

Solid phase peptide synthesis (SPPS) of peptide with Cy5 conjugates

Peptide synthesis was performed from C-terminus to N-terminus using standard Fmoc SPPS peptide chemistry. 300mg Rink Amide resin (aapptec) was pre-swelled in N-methyl-2-pyrrolidone (NMP, Fisher Scientific) for 2 hours prior to synthesis. Before each coupling, Fmoc group was deprotected by treatment of three washes of 20% piperidine (VWR) in NMP for 30 seconds, 2 minutes, and 20 minutes. Coupling of each amino acid was performed with 2 equivalents of Fmoc-protected amino acid (ChemPep), 2 equivalents of (2-(7-Aza-1H-benzotriazole-1-yl)-1,1,3,3-tetramethyluronium hexafluorophosphate) (HATU, ChemPep), and 10 equivalents of diisopropylethylamine (DIPEA, MilliporeSigma) for over 2 hours. NMP washes were performed between each step. After coupling of the peptide was completed, Cy5 fluorescent dye was coupled with 1.3 equivalents of Cy5 carboxylic acid, 1.3 equivalents of HATU, and 2 equivalents of DIPEA for overnight, and deprotected by 20% piperidine in NMP. Peptide-dye conjugates were cleaved off the resin by treatment with a 95:5:5 ratio of trifluoroacetic acid (TFA, MilliporeSigma) : water : triethylsilane (TES, MilliporeSigma) for 2 hours with shaking. The cleavage solution was precipitated into pre-chilled anhydrous diethyl ether (Fisher Scientific), pelleted by centrifugation, and air-dried to remove the remaining solvent. The precipitate was resuspended in dimethyl sulfoxide (DMSO, MilliporeSigma) for purification.

Purification and characterization of synthesized peptide-Cy5 conjugates

Synthetic peptide-dye conjugates in DMSO were purified via prep-scale high-performance liquid chromatography (HPLC) Dionex U3000 with a reverse-phase C18 column

(Phenomenex). Gradients were prepared with distilled water and HPLC grade acetonitrile (VWR) with 0.1% TFA in both. A gradient of 10%-65% acetonitrile in 25min was used and fractions were collected based on absorbance at 280nm and 660nm. Peptides were characterized after purification by matrix-assisted laser desorption ionization time-of-flight (MALDI-TOF) mass spectrometry with Autoflex (Bruker). Product fractions were collected, lyophilized, and reconstituted in DMSO for quantification prior to assays. Peptide-dye conjugates were quantified by determination of extinction coefficients and measurement of absorbance at 280nm and 660 nm on Nanodrop 2000 UV-Vis spectrophotometer (ThermoFisher).

2.3 Peptide-directed fluorescent staining in retinal tissue

The retina has a complex structure, with 10 layers of cells observed microscopically (**Figure 2.3**). There are four main layers that play the most important roles: (1) a monolayer of retinal pigment epithelium (RPE) that supports the neural retina nutritionally and immunologically; (2) photoreceptors, including rods and cones, as light sensing cells; (3) bipolar neurons and ganglion cells that transmit messages to nerve systems; and (4) Müller cells as living optical fibers to support the framework⁴³. In order to investigate risuteganib's preferential binding to certain cell type(s) in the retina, we decided to use peptide-fluorophore conjugate to stain the ocular cross-sections with all cell layers presented on one section. The intensity of fluorescent signals in each cell layer can be compared to show which layer is the potential target for risuteganib.

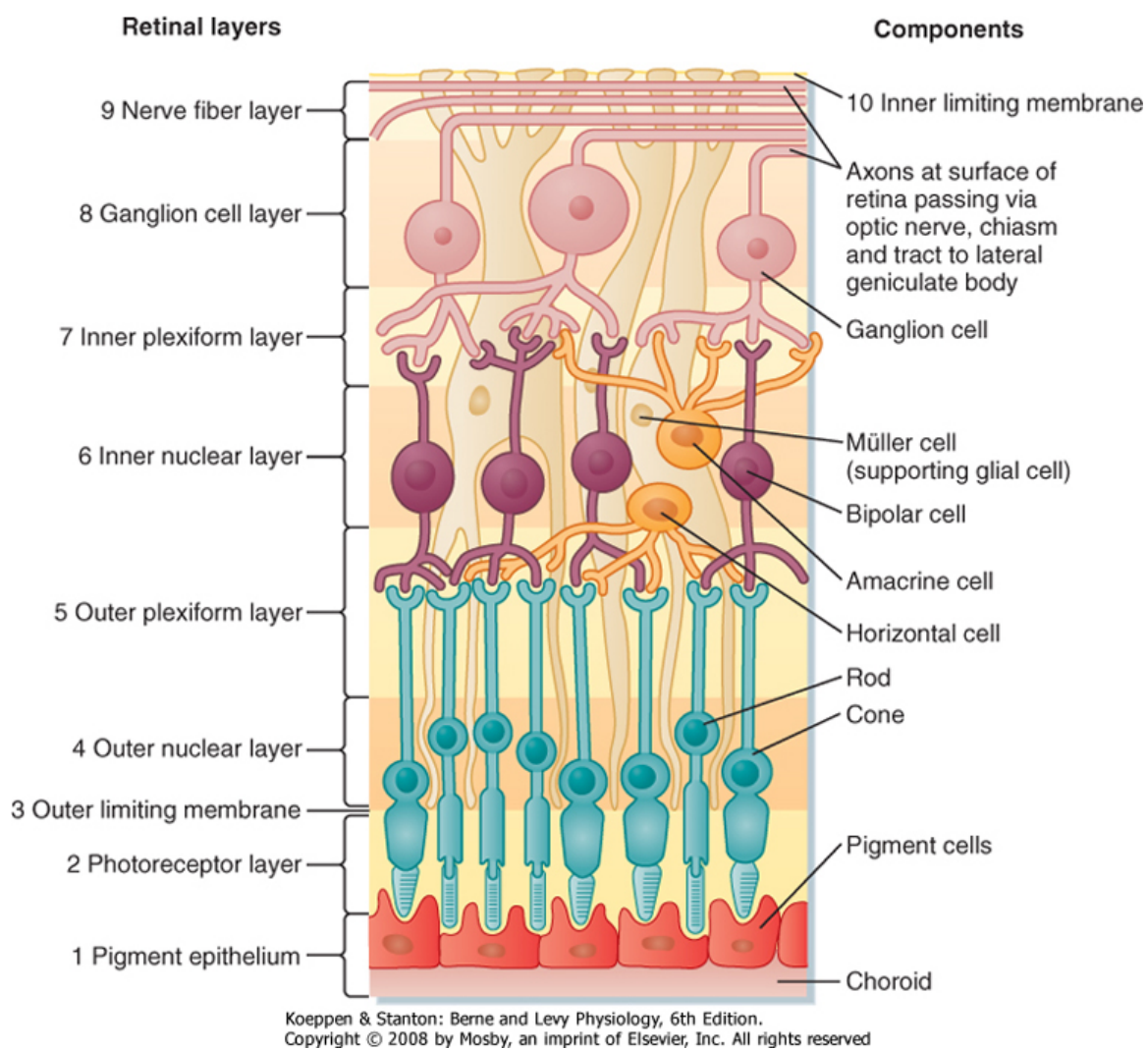
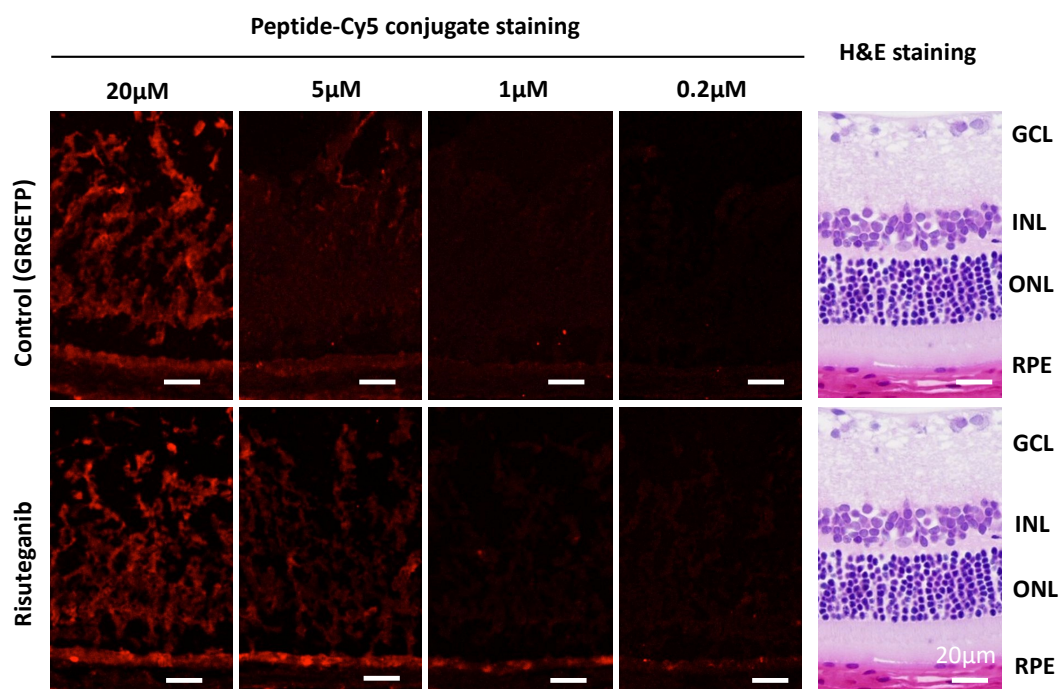


Figure 2.2 Layers of the retina⁴⁵.

2.3.1 Results

To visualize the spatial distribution of risuteganib binding loci in the retina, we stained mouse retina tissue sections with risuteganib-Cy5 at four different concentrations (0.2, 1, 5, 20 μ M). Adjacent serial ocular sections from the same mouse eye were stained with GRGETP-Cy5 as a control (**Figure 2.3A**). At the highest staining concentration (20 μ M), both risuteganib-Cy5 and control GRGETP-Cy5 gave similar extent and distribution of staining the retina, indicating non-specific binding. Lower staining concentrations (0.2-5 μ M) revealed that Risuteganib preferentially stains the retinal pigment epithelium (RPE) relative to GRGETP-Cy5 (other retinal layers show weak, nonspecific staining for both peptides). Confocal micrographs with higher resolution further confirmed the staining of risuteganib-Cy5 on the RPE monolayer (**Figure 2.3B**) These results suggest that the loci of binding of risuteganib are relatively concentrated in the RPE layer of the retina.

A



B

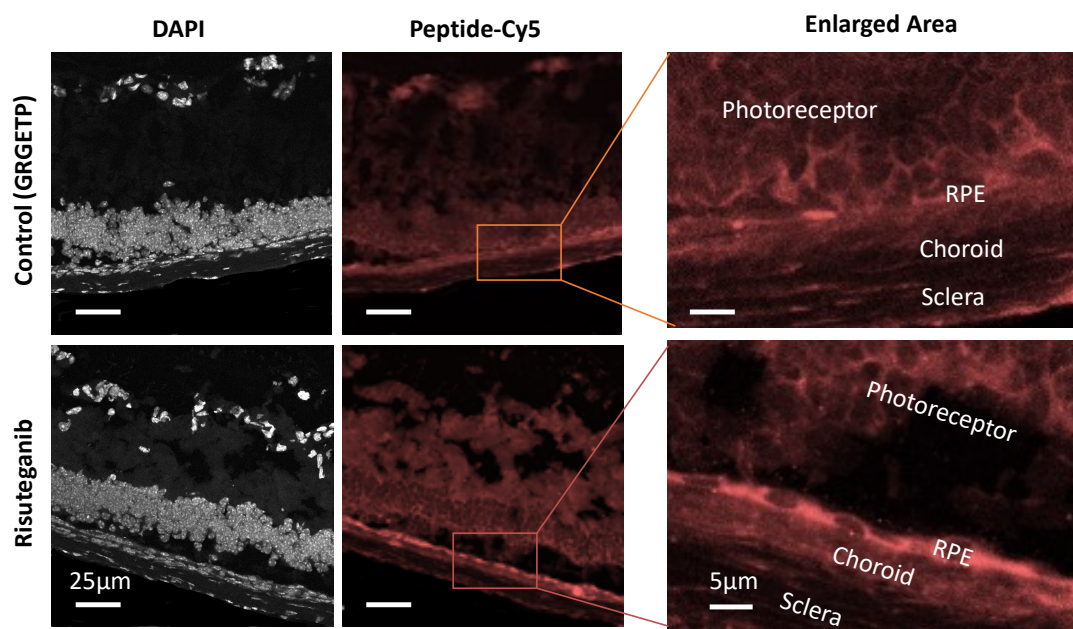


Figure 2.3 Risuteganib preferentially binds to retinal pigment epithelial (RPE) layer.

(A) Microscopic graphs of mouse retinal sections stained by control peptide and Risuteganib fluorophore conjugates (GRGETP-Cy5 and Risuteganib-Cy5) at 0.2, 1, 5, 20 μ M, compared to mouse retina with H&E staining. At concentrations lower than 5 μ M, specific staining by Risuteganib-Cy5 relative to control peptide is observed in the RPE cell layer (B) Higher magnification confocal micrographs of mouse retinal sections confirm the preferential staining of risuteganib-Cy5 to the monolayer of RPE cells. GCL: ganglion cell layer; INL: inner nuclear layer; ONL: outer nuclear layer; RPE: retinal pigment epithelium.

2.3.2 Discussion

Peptide-directed fluorescent labeling is an illuminating approach, which revealed that a monolayer of cells, retinal pigment epithelium (RPE), as the preferential binding loci of risuteganib. The RPE was never thought to be a potential target, as it is far from the original design of risuteganib.

The RPE layer is essential for retinal function. Beyond its optical role (absorbing light so that it is not scattered back into the eye), it is responsible for vital regulatory functions. The RPE regulates transport of ions, water, metabolic end products, and nutrients between the choroidal circulation and the photoreceptor layer. Further, the RPE maintains photoreceptor excitability by phagocytosis of the shed photoreceptor outer segments. Finally, the RPE maintains a polarized environment in which the retinal side of the RPE cell layer has appropriate complement growth factors and immunosuppressive factors, excluding proinflammatory cytokines and immune cells that are present in the choroid (**Figure 2.4**)⁴⁵. Interestingly, it also regulates both angiogenic factors, the vascular endothelium growth factor (VEGF), and anti-angiogenic factors, pigment epithelium-derived factor (PEDF), which is the critical balance to maintain retinal hemostasis. In relation to clinical indications in which risuteganib is being tested, there a strong link between RPE dysfunction and the retinal diseases of both AMD and DME.

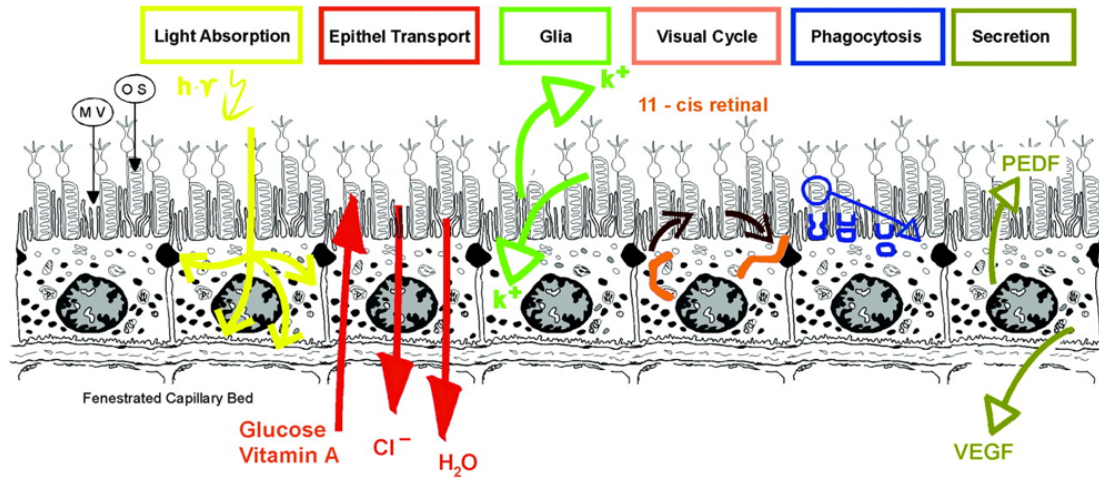


Figure 2.4 Summary of retinal pigment epithelium (RPE) functions⁴⁵. PEDF: pigment epithelium-derived growth factor; VEGF: vascular epithelium growth factor; MV: microvilli; OS: outer segment.

Disruption of RPE functions is implicated in retinal diseases, particular AMD and DME.

As the RPE layer closely interacts with photoreceptors on its retinal side and with endothelial cells and cells of the immune system on its choroidal side, it serves an important role as the blood-retinal barrier (BRB)⁴⁶, which separates the inner space of the eye from the blood stream. It communicates with the immune system by inhibiting the immune reaction in the healthy eye and activating the immune system in the case of disease. In DME and AMD, vascular leakage due to the breakdown of the BRB is the hallmark to the pathogenesis of these retinal diseases^{47,48}. Therefore, it is particularly interesting to observe that risuteganib preferentially interacts with the RPE. Further experiments were conducted to explore hypotheses regarding the possibility that risuteganib might act on the RPE in a way that promotes return to a healthy homeostasis, which could provide improved neuroretinal support and, consequently, better visual functions.

2.3.3 Methods

Staining of mouse retina with peptide-Cy5

Mouse eyes in this study were obtained from two resources: BALB/c (albino) from Sierra for Medical Science, and C57BL/6 (pigmented) from the Office of Laboratory Animal Resources (OLAR) at Caltech. Immediately after receiving the animal tissue, mouse eyes were embedded in glycol-based optimal cutting temperature compound (OCT, Sakura Finetek USA) and flash frozen in liquid nitrogen. Frozen serial sections (10 μ m thick) were cut through the retinal region and mounted on glass slides. Sections were fixed by incubating in 4°C 4% paraformaldehyde for 10 minutes and washed with 10mM phosphate buffered saline (PBS, pH 7.4, ThermoFisher). Tissue sections were permeabilized with 0.1% Triton

X-100 (MilliporeSigma) for 10 minutes, blocked with 5% Bovine Serum Albumin (BSA, MilliporeSigma) in PBS for 1 hour at room temperature or overnight at 4°C, stained with 0.2, 1, 5, or 20µM peptide-Cy5 conjugate in PBS containing 1% BSA for 1 hour at room temperature and washed with 0.5% tween-20 (MilliporeSigma) in PBS three times to remove unbounded labels. Mounting medium Fluoroshield with DAPI (MilliporeSigma) was added onto of each section prior to placing the coverslip on the sections. All images were acquired with a Zeiss LSM 710 confocal microscope.

2.4 ARPE19 as a cell model for retinal pigment epithelium (RPE)

Based on the result from the peptide-directed fluorescent labeling, we hypothesized that risuteganib targets RPE cells, which could be further connected to risuteganib's drug efficacy of enhanced retinal functions observed clinically. To further investigate cellular functions that are difficult to access *in vivo*, we selected an *in vitro* model.

Methods to cultivate the RPE cells *in vitro* have been under development since the 1970s^{49,50}. Cultured RPE cells can be used in a variety of applications, including DME and AMD research⁵¹. Cell models for RPE include immortalized cell lines, iPSC differentiated RPE cells, and cells isolated from human donors or animals⁵¹. The most commonly used cell line, ARPE19, was established from cells isolated from the enucleated globes of a 19-year-old male human donor⁵². Although cultivated RPE cells share similar orientation, configuration, and morphology as those found in the tissue, it is important to remember that cell lines are altered with respect to proliferation profiles, loss of pigmentation, low cell-substrate adhesion rates, and some alterations in cell morphology. Indeed, a cell culture protocol that

appropriately differentiates RPE cells is essential to mimic the behaviors, functions, and genomic profiles of native cells. Here, we adopted the protocol developed in the Coffey group at University College London⁵³, which showed that appropriately differentiated ARPE19 cells regain phenotype and gene expression profiles similar to native RPE cells⁵⁴. The protocol features: (1) cultivating cells in transwell, which allows mass transport from top and bottom to mimic epithelial cell environment, (2) growing cells in culture medium with high glucose and pyruvate to induce differentiation, and (3) culturing cells for over 4 weeks to allow appropriate differentiation.

2.4.1 Results

Following the protocol of the Coffey group, ARPE19 cells developed the characteristic RPE phenotype, both in cell morphology and expressing the RPE-specific protein markers RPE65 and cellular retinaldehyde-binding protein (CRALBP) (**Figure 2.5**). The commercially available ARPE19 cells from ATCC do not have RPE phenotypic morphology and protein profiles due to extensive passages *in vitro*. APRE19 cells under regular microplate culturing environment have elongated shapes and express little or none of the RPE-specific protein markers, RPE65 and CRALBP. In comparison, 30-day differentiated ARPE19 cells cultivated in laminin-coated transwells exhibit roughly hexagonal shapes, and express high levels of both protein markers. Based on the result of §2.3, we tested the properly differentiated ARPE19 cells *in vitro* for specific binding of risuteganib-Cy5, compared to control GRGETP-Cy5 (**Figure 2.6**). Risuteganib showed higher binding to the ARPE19 cells than the control peptide.

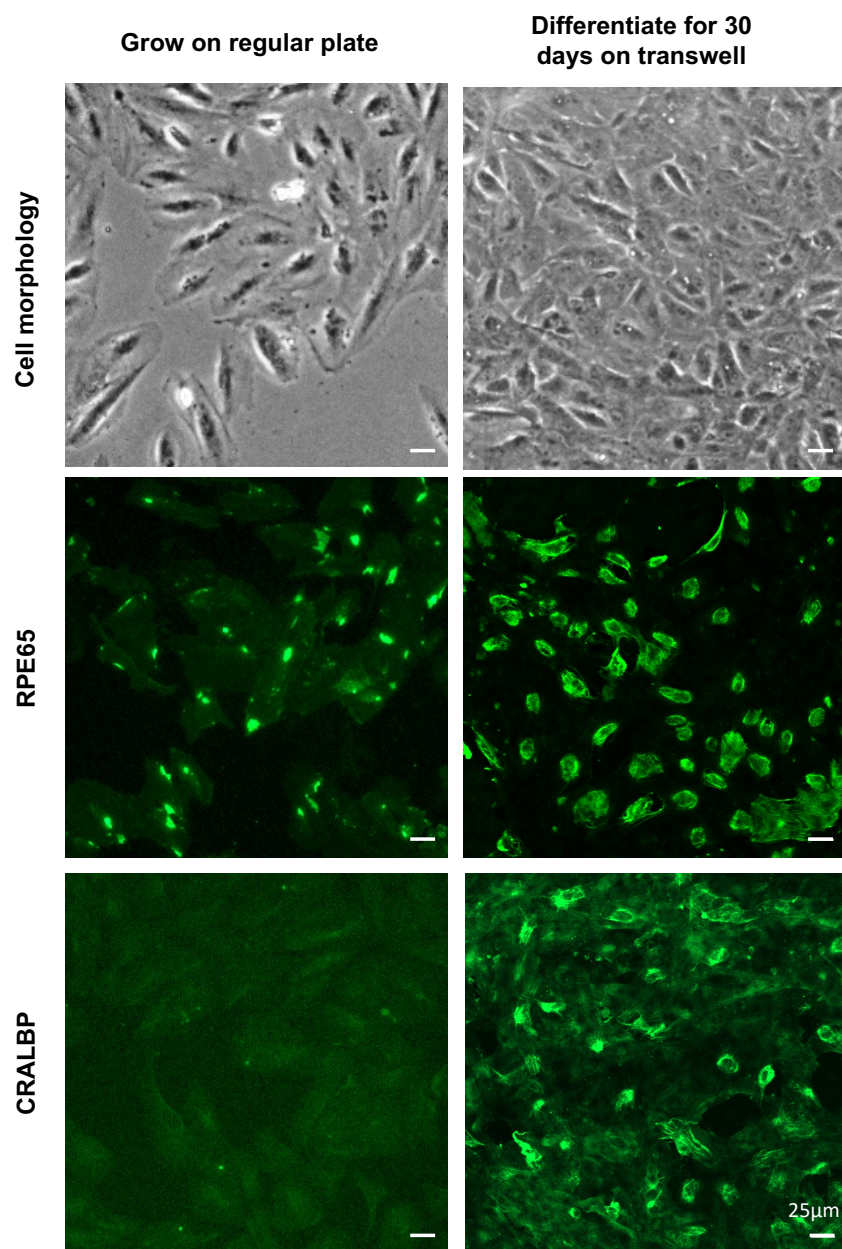


Figure 2.5 ARPE19 cells develop RPE phenotype characteristics and express RPE-specific protein markers, RPE65 and CRALBP. The 30-day differentiated ARPE19 cells (on the right) were compared to cells plated on regular microplate for 2 days (on the left).

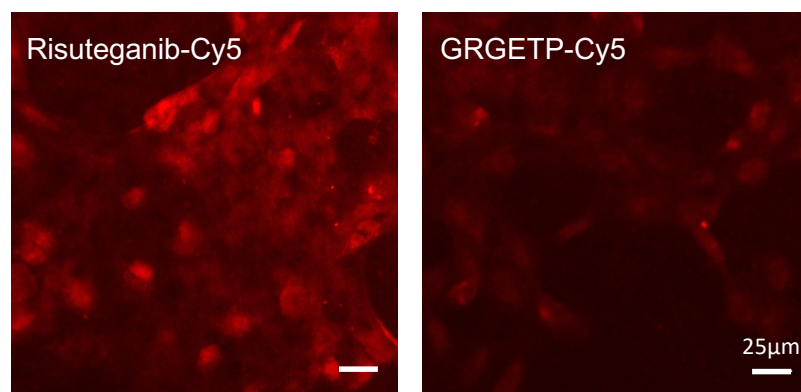


Figure 2.6 Appropriately differentiated ARPE19 cells are specifically stained with **risuteganib-Cy5**. After 30 days of differentiation on transwells, ARPE19 cells stained with 5µM Risuteganib-Cy5 (on the left) showed more fluorescent signals than control GRGETP-Cy5 (on the right).

2.4.2 Discussion

With the same peptide-fluorophore conjugates used in §2.3 tissue labeling, we found it consistent that 5 μM risuteganib showed stronger binding onto differentiated ARPE19 cells, compared to control peptide. The result indicates that ARPE19 cells with proper differentiation may provide an *in vitro* model to study effects of risuteganib on RPE cells. Encouraged by specific binding, we next examine the effects of risuteganib on cell function.

2.4.3 Methods

ARPE19 cell culture and differentiation into polarized phenotype

ARPE19 cells (P20) were purchased from American Type Culture Collection (ATCC) and first grown to P23 in Dulbecco's Modified Eagle's Medium/Nutrient Mixture F-12 (DMEM:F12, Thermo Fisher Scientific) with 10% fetal bovine serum (FBS, Thermo Fisher Scientific). Early passage ARPE19 cells grew as non-pigmented, epithelioid, non-polarized cells, and were passed to regular glass-bottom plates (Ted Pella) for control study as 2-day cultivated ARPE19 cells. For proper differentiation into the polarized phenotype, ARPE19 were seeded in 24mm transwells with a 0.4 μm pore polyester membrane insert (Corning) coated with laminin (VWR). Cells were then cultured in an enriched medium, DMEM with 1% FBS, 4.5g/L glucose, and 1mM pyruvate (Thermo Fisher Scientific), for 30 days. Medium was changed twice weekly.

Immunolabeling of ARPE19 cells to identify the phenotype

ARPE19 cells, either from 2-day cultivation on regular plate or with 30-day differentiation on transwells were washed with 4°C PBS three times and fixed with 4% paraformaldehyde for 10 minutes. For differentiated cells, the transwell membrane containing the fixed cells was separated from the insert. Cells were permeabilized with 0.1% Triton X-100 (MilliporeSigma) for 10 minutes, followed by overnight blocking in 5% Bovine Serum Albumin (BSA, MilliporeSigma) at 4°C. ARPE19 cells were immunostained with either mouse anti-human RPE65 mAb (Thermo Fisher Scientific) or mouse anti-human CRALBP mAb (Thermo Fisher Scientific), followed by goat anti-mouse IgG (H+L) alexa fluor 488. After PBS wash, coverslip and mounting medium Fluoroshield with DAPI (MilliporeSigma) were added onto the transwell membrane or regular plate. All images were acquired with a Zeiss LSM 710 confocal microscope.

Fluorescent staining of Risutagnib-Cy5 and GRGETP-Cy5 on differentiated ARPE19 cells

ARPE19 cells with 30-day differentiation were washed with cold PBS three times and fixed with cold 4% paraformaldehyde for 10 minutes. Transwell membranes containing the fixed cells were separated from the insert and cells were permeabilized with 0.1% Triton X-100 (MilliporeSigma), followed by overnight blocking in 5% Bovine Serum Albumin (BSA, MilliporeSigma). ARPE19 cells were then stained with 5 μ M Risutagnib-Cy5 or RGE-Cy5 for an hour. Coverslip and mounting medium Fluoroshield with DAPI (MilliporeSigma) were added onto the transwell membrane. All images were acquired with a Zeiss LSM 710 confocal microscope.

2.5 Risuteganib protects ARPE19 cells against oxidative stress

To explore whether preferential binding of risuteganib on RPE is related to its cellular function, we examine the drug interaction with differentiated ARPE19 cells. RNA-sequencing study done by Dr. Zach Shao in our group found no or limited effects of risuteganib in healthy animals, while significant effects were observed in a disease-related animal model⁵⁵. Therefore, we sought a diseased-related condition to impose our cell model.

Elevated oxidative stress is an important contributing factor to retinopathy, and RPE layer is thought to be a critical site of oxidative injury in DR and AMD⁵⁶⁻⁵⁸. Clinical pathology studies indicate that oxidative damage to the RPE layer is observed early in the disease development⁵⁹. Following an established protocol for *in vitro* studies of oxidative stress in RPE cells⁶⁰, we induced oxidative stress in the ARPE19 *in vitro* model, using tert-butyl hydroperoxide (tBH).

2.5.1 Results

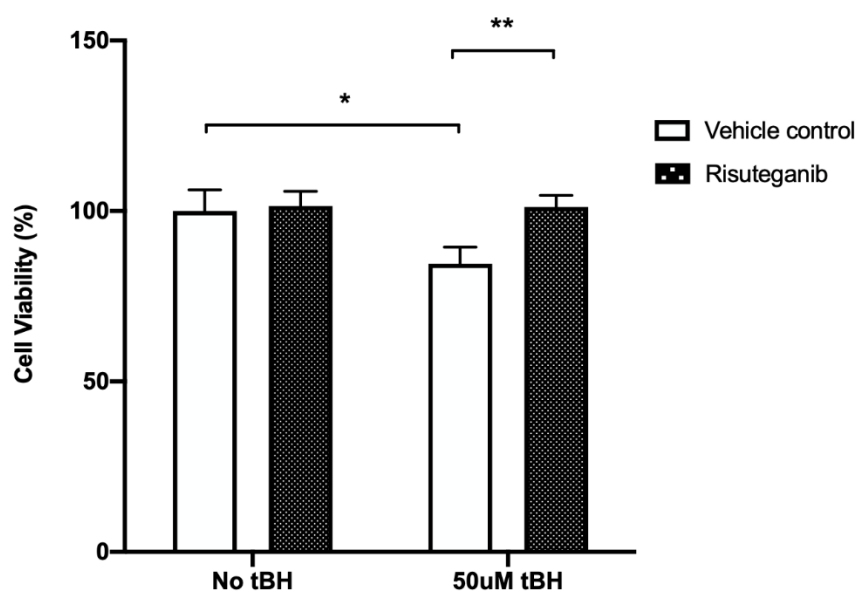
To mimic the oxidative stress associated with retinal disease conditions, we induced a 1-hour exposure of 50 μ M tert-butyl hydroperoxide (tBH) to 30-day differentiated ARPE19 cells. Using the culture condition that produces ARPE19 with the correct phenotype (§2.4), we pre-treated the cells for 24hr with either 300 μ M risuteganib prior to oxidative challenge. Oxidative stress was imposed by replacing media with fresh media containing 50 μ M tBH; in the treated group of wells, 300 μ M risuteganib was also included in the medium.

To evaluate protection against oxidative stress, cell viability was measured using an NADH-dependent WST-1 cell proliferation assay. The reduced viability due to 50 μ M tBH stress in the control wells (100% for no tBH versus 85% for 50 μ M tBH, $p=0.0274$, $N=3$) is significantly mitigated in the risuteganib treated wells (85% for 50 μ M tBH versus 101% for 50 μ M tBH with 24hr 300 μ M risuteganib pretreatment, $p=0.0083$, $N=3$) (**Figure 2.7A**).

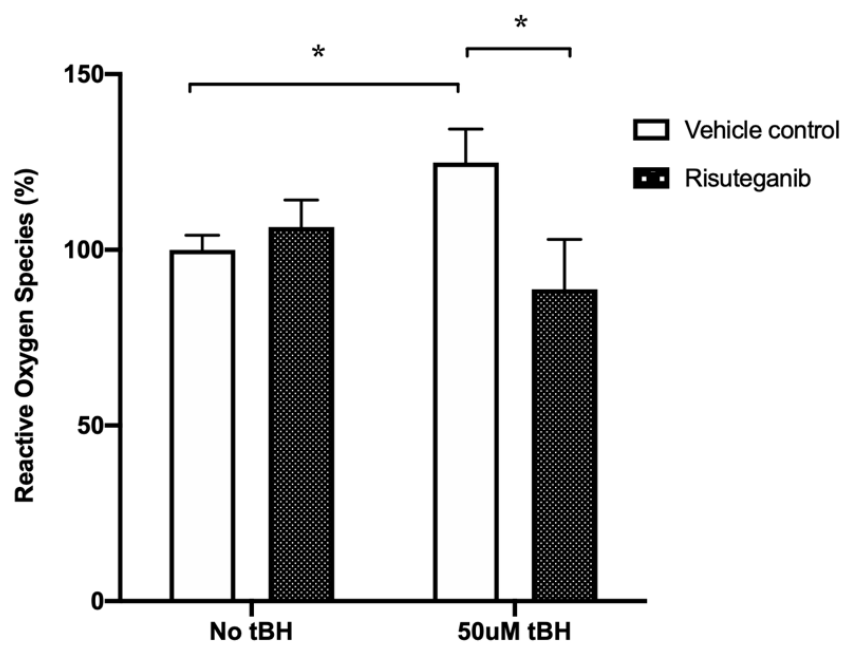
As reactive oxygen species (ROS) are important indicators of intracellular oxidative stress, a cell-permeant fluorescent dye (H2DCFDA) was used to measure ROS levels. Relative to control cells that are not exposed to tBH, ROS levels are elevated in cells exposed to tBH (100% for no tBH versus 125% for 50 μ M tBH, $p=0.0146$, $N=3$). 24hr pretreatment with risuteganib produces a significant reduction of intracellular ROS (125% for 50 μ M tBH versus 89% for 50 μ M tBH with 24hr 300 μ M risuteganib pretreatment, $p=0.0219$, $N=3$) (**Figure 2.7B**).

Oxidative stress is associated with damage of mitochondrial DNA, proteins, and lipids^{61,62}, resulting in impaired mitochondrial function, revealed by a decrease in mitochondrial membrane potential⁶³. In our ARPE19 model, oxidative stress from tBH significantly decreases mitochondrial membrane potential (100% for no tBH versus 86% for 50 μ M tBH, $p=0.0284$, $N=3$), while risuteganib significantly preserve the mitochondrial membrane potential (86% for 50 μ M tBH versus 111% for 50 μ M tBH with 24hr 300 μ M risuteganib pretreatment, $p=0.0079$, $N=3$) (**Figure 2.7C**).

A



B



C

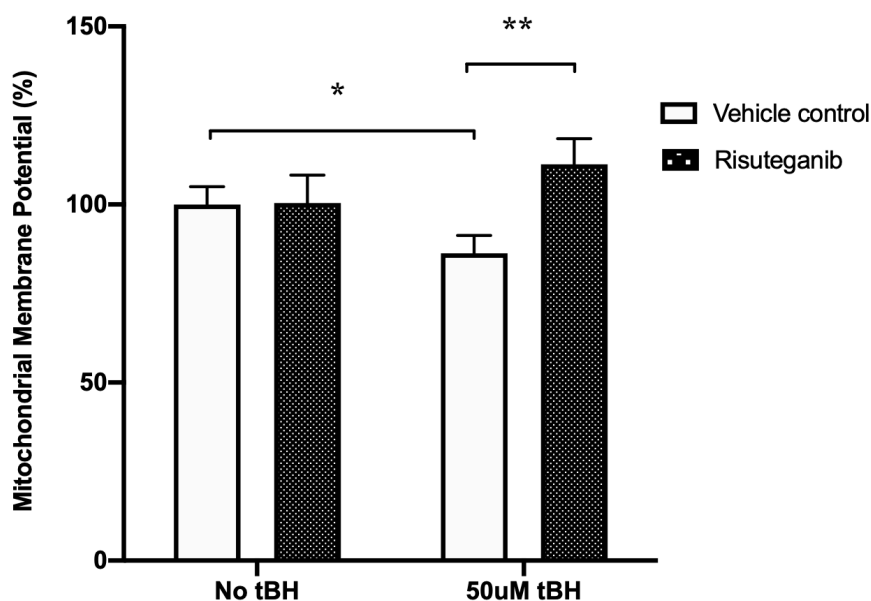


Figure 2.7 Risuteganib pre-treatment protects ARPE19 cells under oxidative stress.

ARPE19 cells were treated with 50 μ M tert-butyl hydroperoxide (tBH) for 1 hour. Under this oxidative stress, cells showed (A) reduced cell viability, (B) increased reactive oxygen species, and (C) loss of normal mitochondrial membrane potential. To test the risuteganib drug effect on stressed cells, APRE19 cells were pre-treated with 1x clinical dosage, 300 μ M risuteganib for 24 hours. Risuteganib protects ARPE19 cells under tBH stress as evidenced by reduced cell apoptosis, lower intracellular ROS, and preserved mitochondrial membrane potential. Data are mean \pm SD. n.s. $p > 0.05$ versus corresponding untreated group.

2.5.2 Discussion

Our results in unstressed cell conditions (no tBH) are consistent with previous RNA-seq observation in animal model studies, that risuteganib showed no significant effect on unstressed animals. The disease-related oxidative stress induced by tBH showed significant impact on reducing cell viability, increasing ROS production, and reducing mitochondrial potential, while risuteganib showed protective effect for ARPE19 by reversing these adverse effects. With 24hr pretreatment of risuteganib, tBH-stressed ARPE19 cells showed enhanced cell viability, lower ROS, and higher mitochondrial potential, indicating that risuteganib may protect cells through moderating intracellular ROS. As mitochondria is one of the main sources of ROS production and the main target for oxidative stress, ROS may be moderated by the protective effect of risuteganib to mitochondria.

2.5.3 Methods

Cell culture, oxidative stress application and treatment of risuteganib

Following the previously described protocol (Chapter 2.4.4), ARPE19 cells were differentiated in transwells for 30 days, and then passed to a 96-well plate. ARPE19 cells in the 96-well plate were cultivated in DMEM:F12 1:1 mixture medium containing 10% FBS for 2 days before assay. Cells were exposed to oxidative stress, 50 μ M tert-butyl hydroperoxide (tBH, MilliporeSigma, chosen over hydrogen peroxide based on the greater stability of tBH) for 1 hour. For pre-treatment, cells were treated with 300 μ M risuteganib 24 hours before exposure to 50 μ M tBH. 300 μ M risuteganib was selected to match 1x clinical dosage, calculated based on 1mg clinical dosage per injection, diluted in 5mL human

vitreous. After the 1-hour tBH exposure was finished, cells were washed twice with PBS containing Ca^{2+} and Mg^{2+} , and assessed by the following assays.

The protocol was developed by tBH concentrations of 50, 100, 200, and 400 μM , duration of oxidative stress of 1hr and 4hr, and treatment modes of concurrent treatment, 4hr or 24hr pretreatment; the greatest statistical significance was observed for 24hr pretreatment followed by 1hr 50 μM tBH stress.

WST-1 assay

WST-1 reagent is used for quantification of cell proliferation and viability in cell populations. The stable tetrazolium salt WST-1 is cleaved to a soluble formazan by a complex cellular mechanism which is largely dependent on the glycolytic production of NAD(P)H in viable cells. This NAD(P)H-dependent assay reflects the number of viable cells present in cultures. After cells were exposed to oxidative stress, rinsed with PBS, and replaced with cell culture medium, WST-1 reagent was added to the cell culture medium at 1:10 ratio and cultured for 1 hour at 37°C. Absorbance signal at 440nm was measured on Flexstation3 microplate reader. Baseline absorption from the background and medium was subtracted to isolate the contribution of the cells. Absorbance ratios were normalized to untreated 100%.

Reactive oxidative species (ROS) assay

ROS assay was performed with cell-permeant 2',7'-dichlorodihydrofluorescein diacetate (H2DCFDA), a chemically reduced form of fluorescein. Upon cleavage of the acetate groups

by intracellular esterases and oxidation, the nonfluorescent H2DCFDA is converted to the highly fluorescent 2',7'-dichlorofluorescein (DCF).

After cells were exposed to oxidative stress, rinsed with PBS, and replaced with cell culture medium, H2DCFDA reagents were added to the cell culture medium at 10 μ M. After 30min incubation at 37°C, the dye solution was removed and replaced with PBS buffer. The fluorescent signal was measured on Flexstation3 microplate reader with EX filter at 482nm and EM filter at 520nm. Fluorescent signal ratios were normalized to untreated 100%.

Mitochondrial Membrane Potential

The mitochondrial membrane potential was measured by JC-1 kit (Biotium) that contains 5,5',6,6'-tetrachloro-1,1',3,3'-tetraethyl-benzimidazolyl-carbocyanine-iodide, a cationic dye that fluoresces red within the mitochondria of healthy, live cells. In the stressed or apoptotic cells, the mitochondrial membrane potential collapses and the cationic dye fluoresces green.

After cells were exposed to oxidative stress and rinsed with PBS, cells were incubated with JC-1 reagent working solution at 37°C for 15 minutes. After staining, the JC-1 reagent was removed, and cells were washed twice with PBS. The red fluorescence (live cells) was read with EX filter at 550nm and EM filter at 600nm. The green fluorescence (apoptotic cells) was read with EX filter at 485nm and EM filter at 535nm. The changes in mitochondrial membrane potential were calculated by the ratio of red to green fluorescence. Results were normalized to untreated 100%.

2.6 Potential connection between the binding loci to drug efficacy in RPE

An unbiased search for the retinal cells that preferentially bind risuteganib led us to the RPE. Although this location was unanticipated, it is intriguing as RPE dysfunction is one of the hallmarks for both retinal diseases for which risuteganib is in clinical trials, diabetic retinopathy and age-related macular degeneration.

To further study the effects of risuteganib at a cellular level, we used properly differentiated ARPE19 cells *in vitro* and subjected them to disease-related oxidative stress. Risuteganib pretreatment protects ARPE19 by increasing cell survival, reducing ROS production, and maintaining mitochondrial integrity. Based on the results in the stressed cell model, we started to form a hypothesis about the mechanism of action of risuteganib on RPE cells. The protective effect of risuteganib on RPE under oxidative stress may result from protection of the mitochondrial function. As mitochondrial damage in RPE cells plays an important role in disease pathogenesis, the next step of our journey was to explore risuteganib drug effect on mitochondria.

RISUTEGANIB PROTECTS MITOCHONDRIA THROUGH REGULATION OF OXIDATIVE PHOSPHORYLATION METABOLISM

3.1 Energetic requirements of the retinal pigment epithelium (RPE)

The retina shares the high energy demand of central nervous system, which is normally matched with a large supply of metabolites⁶⁴. The characteristics of high energy and high metabolic demands make the retina vulnerable to metabolic dysregulation. Diabetic retinopathy (DR) starts with excess glucose, while age-related macular degeneration (AMD) is thought to be caused by accumulation of metabolic by-products^{65,66}.

One of the hallmarks for both diseases is the disruption of the RPE monolayer. The RPE layer has one of the highest demands for ATP in the retina⁶⁷, consumes a substantial portion of the energy needed to support photoreceptor functions. It absorbs and degrades damaged disks shed from the outer segments of photoreceptor cells, restores the photopigment in cones, and transports metabolites to the retina⁶⁸. A number of recent studies have highlighted the critical role of mitochondria within RPE cells maintaining the homeostasis of the retina^{69–71}. In disease development, dysfunction of RPE mitochondria results in insufficient ATP production, which impacts on biosynthesis and cell functions.

Consequently, mitochondria recently emerged as a promising therapeutic target to treat retinal diseases⁷¹. Based on the evidence we uncovered that risuteganib may act on the

mitochondria in RPE cells, we continued our journey to investigate the possibility of mitochondrial targeting by risuteganib (§3.2) and to search for the molecular mechanism by which risuteganib alters the mitochondrial bioenergetics (§3.3, §3.4). The evidence we collected help us form a new hypothesis on the MOA of risuteganib that may explain the its promising clinical effects (§3.5).

3.2 Drug effect on mitochondrial respiration in RPE cells

Mitochondria are the powerhouse of eukaryotic cells. They produce ATP, the chemical energy for various bio processes, through respiration, and regulate cellular metabolism⁷². The production of ATP is done by oxidizing pyruvate, and NADH, which are produced in the cytosol. Hence it is named “oxidative phosphorylation” or “OXPHOS”. Oxygen-dependent cellular respiration, known as aerobic respiration, provides most of the energy required by the cells. When oxygen is limited, the glycolytic products will be metabolized by anaerobic fermentation, a process that is independent of the mitochondria. The yield of ATP from glucose and oxygen is approximately 13-times higher during aerobic respiration compared to fermentation (**Figure 3.1**).

Based on the central role of RPE mitochondrial malfunctions in retinal diseases and on our observations of risuteganib’s ability to protect RPE mitochondria, we evaluate the effect of risuteganib on mitochondrial bioenergetics. To characterize the effect, we collaborated with Dr. Cris Kenny at UC Irvine, an expert in studying mitochondrial function of RPE cells in retinal diseases. We measured the oxygen consumption rate (OCR) and extracellular

acidification rate (ECAR) in ARPE19 cells undergoing a mitochondria stress test (Seahorse XF cell mito stress test).

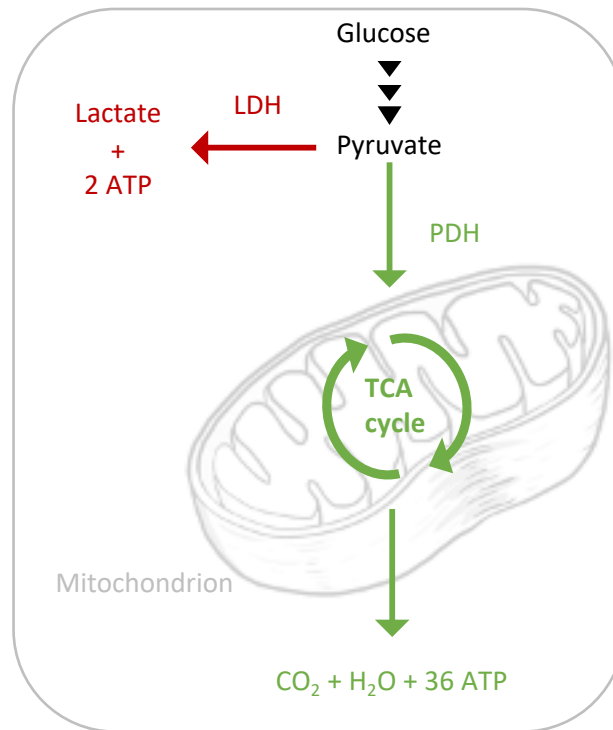


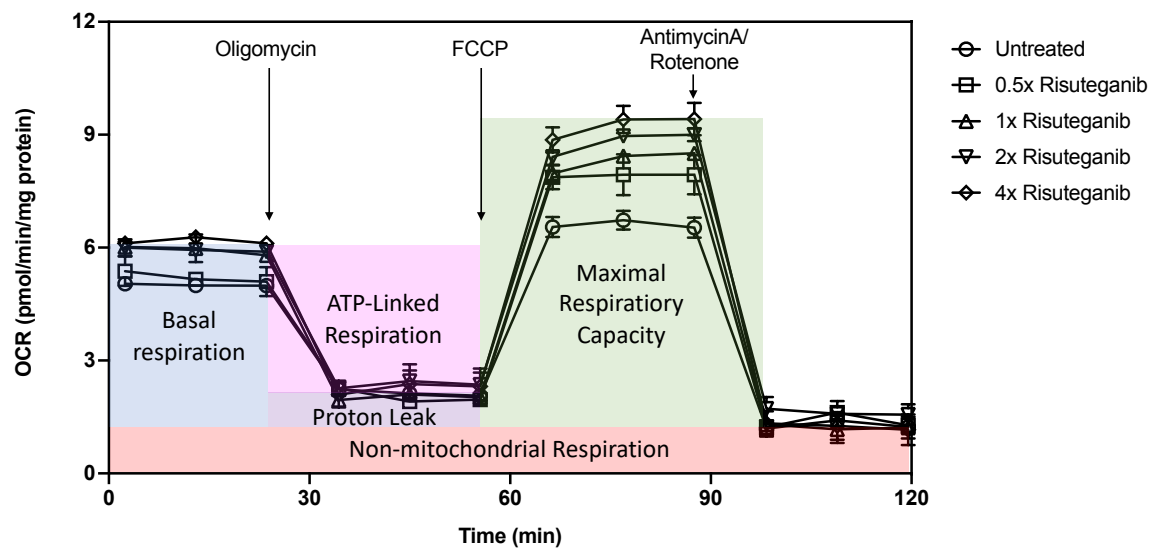
Figure 3.1 ATP production from aerobic respiration is much higher than anaerobic glycolysis in mitochondria. LDH: lactate dehydrogenase; PDH: pyruvate dehydrogenase; TCA: tricarboxylic acid cycle.

3.2.1 Results

The OCR value measured in the Seahorse XF cell mito stress test (**Figure 3.2A**) prior to introducing any active agent represents the basal respiration, that after oligomycin injection showed the amount of oxygen consumption linked to ATP production, and that after FCCP injection denotes the maximal mitochondrial respiratory capacity of the cells. The final injection of antimycinA and rotenone inhibits the flux of electrons in the mitochondria, such that the OCR reading is due to nonmitochondrial oxygen consumption by cytosolic oxidase enzymes. The ECAR value measured reflects lactate production and is used as an index of glycolysis (**Figure 3.3A**).

In the dose-dependent assay, ARPE19 cells incubated with different concentrations of risuteganib showed significant increases of OCR relative to untreated cells: basal respiration (1x clinical dosage $p=0.026$, 4x clinical dosage $p=0.034$, $N=3$), maximal respiratory capacity (1x clinical dosage $p=0.009$, 2x clinical dosage $p=0.012$, 4x clinical dosage $p=0.016$, $N=3$), and ATP-linked respiration (1x clinical dosage $p=0.009$, 4x clinical dosage $p=0.034$, $N=3$) (**Figure 3.2B**). Meanwhile, there was no significant difference in ECAR values (**Figure 3.3B**).

A



B

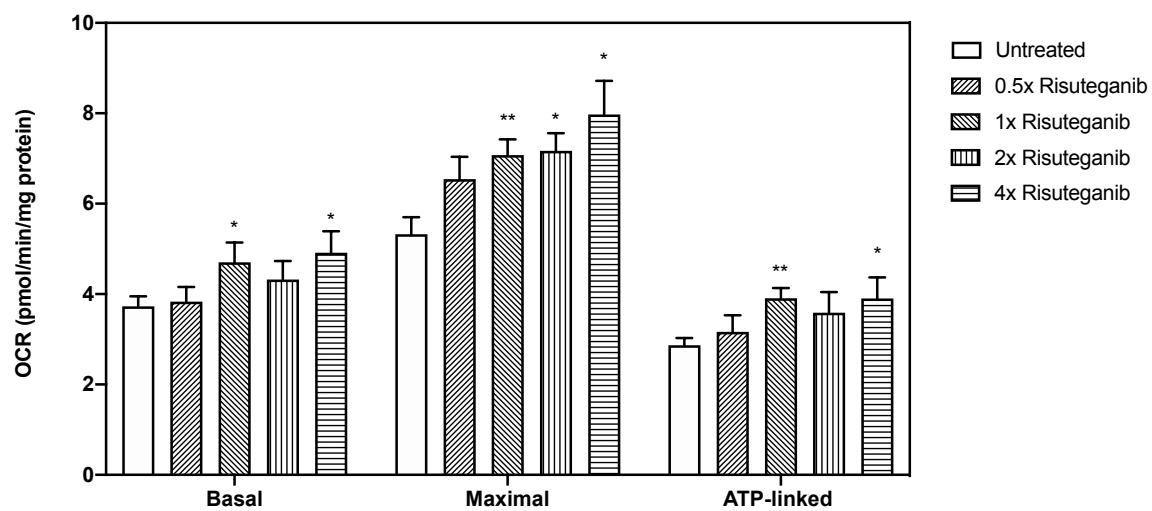
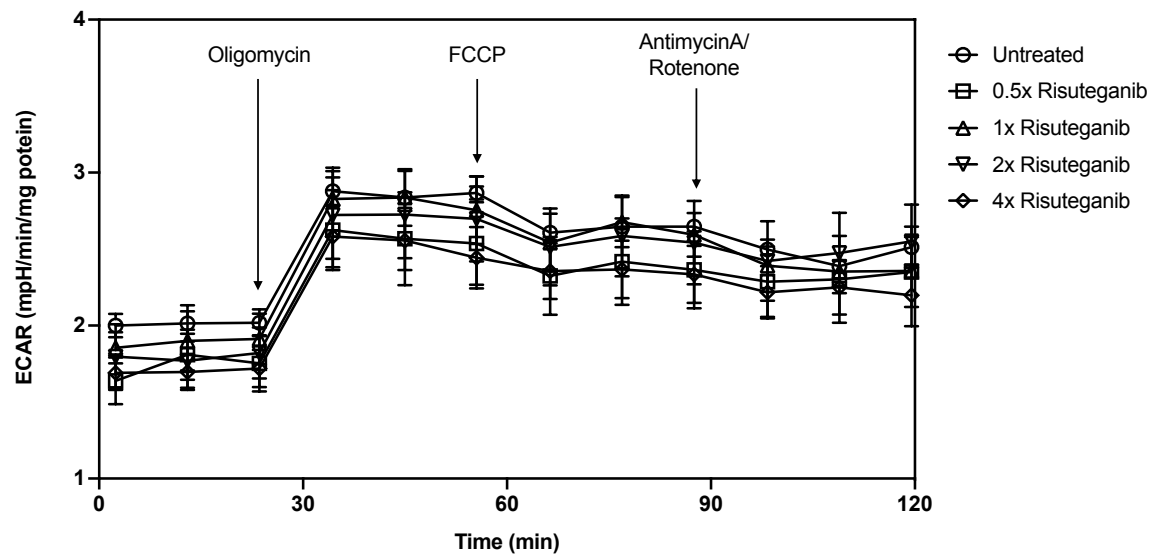


Figure 3.2 Risuteganib increases cellular oxidative phosphorylation in ARPE19 cells.

ARPE19 were incubated with assay media containing 0 (untreated), 0.5x, 1x, 2x, and 4x clinical dosages of Risuteganib for 1 hour at 37°C before the assay. The oxygen consumption rate (OCR) was determined using Seahorse XF-24 metabolic flux analyzer. (A) The changes of OCR were recorded in response to the sequential administration of oligomycin (1µM), FCCP(0.5µM), and antimycinA/rotenone (1 µM) to ARPE19 cells for each group. (B) Risuteganib at different clinical dosages increased basal respiration, maximal respiratory capacity, and ATP-linked respiration. Data are mean ± SD. *p<0.05, **p<0.01 versus corresponding untreated group.

A



B

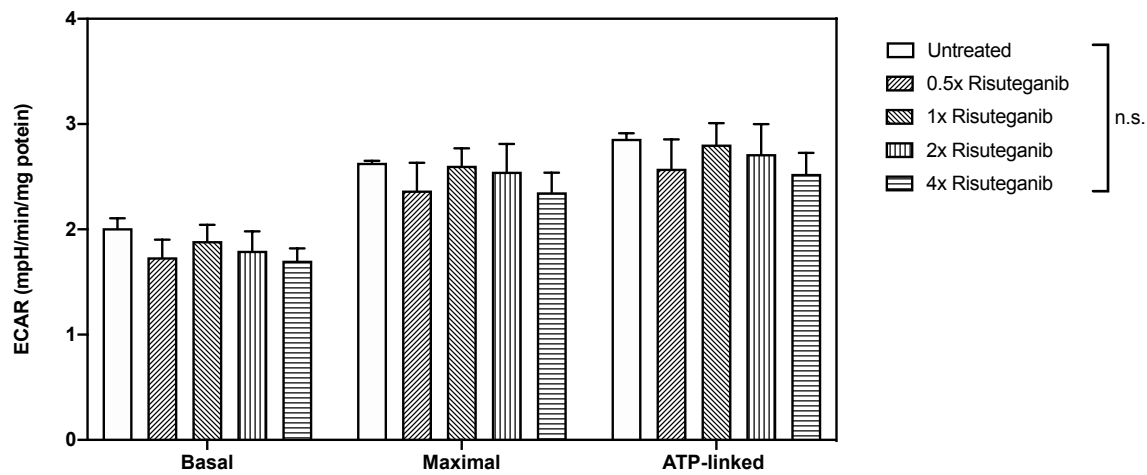


Figure 3.3 No significant effect of Risuteganib on glycolysis in ARPE19 cells.

ARPE19 were incubated with assay media containing 0 (untreated), 0.5x, 1x, 2x, and 4x clinical dosages of Risuteganib for 1 hour at 37°C before the assay. The extracellular acidification rate (ECAR) was determined using Seahorse XF-24 metabolic flux analyzer.

(A) The changes of ECAR were recorded in response to the sequential administration of oligomycin (1 μ M), FCCP (0.5 μ M), and antimycinA/rotenone (1 μ M) to ARPE19 cells for each group. (B) Risuteganib at the different clinical dosages showed no significant effect on glycolysis. Data are mean \pm SD. n.s. $p > 0.05$ versus corresponding untreated group.

3.2.2 Discussion

Mitochondrial energy production is essential to cell survival. Anaerobic respiration, with only 2 ATP produced per pyruvate, is activated during the period when cells are under stress, such as hypoxia. Anaerobic metabolism is also used to route carbons to biosynthesis. For example, cell proliferation during angiogenesis is associated with elevated anaerobic metabolism at the expense of oxidative phosphorylation (OXPHOS)⁷³, which can be a drug target for treating blinding retinal disease.

The present study provides evidence that an increase in mitochondrial bioenergetics may be involved in the risuteganib drug effects. We found that risuteganib treatment significantly increased the oxygen consumption rate in a dose-dependent manner, in both basal respiratory and maximal respiratory capacities (in a dose-dependent manner), and most interestingly, ATP-linked respiration in the mitochondria, while having no statistically significant effect on glycolysis. The increase in ATP-linked respiration indicates that risuteganib treatment increases ATP production in RPE mitochondria, which may be associated with the protective effect of risuteganib on RPE cells under oxidative stress.

Based on this observation, we continued to look into the pathways and proteins associated with OXPHOS in cellular energy production seeking the molecular interaction(s) of risuteganib that give rise to the observed effects on mitochondrial bioenergetics.

3.2.3 Methods

Mitochondrial respiration measurement

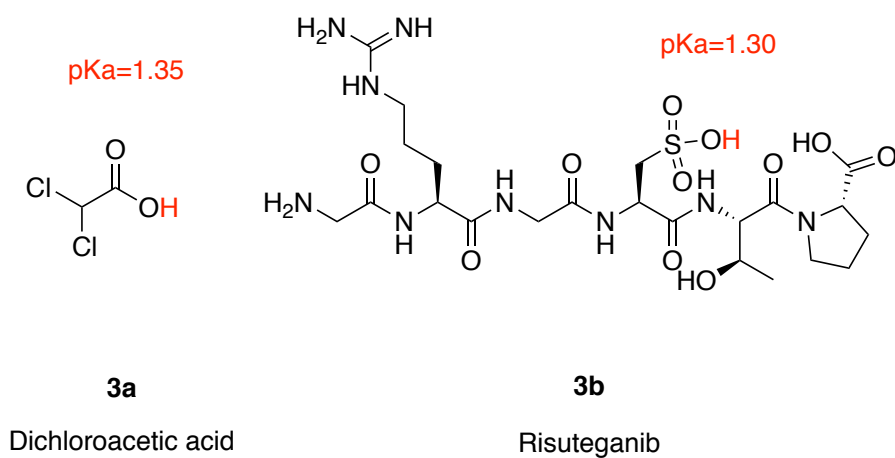
Mitochondrial respiration was assessed using a Seahorse XF24 Extracellular Flux Analyzer (Agilent). ARPE-19 cells were seeded on Seahorse XF-24 plates at a density of 80,000 cells/well and cultured in DMEM:F12 medium with 10% FBS for 24 hours. The sensor cartridge was hydrated with a calibration buffer 1 day prior to each experiment. Each well was washed once with assay medium, formulated with DMEM solution containing 25 mM glucose (MilliporeSigma), 1 mM sodium pyruvate (MilliporeSigma), and 2 mM GlutaMax (ThermoFisher Scientific). It was replaced with assay medium supplemented with 0 (untreated), 0.125mg/mL (0.5x clinical dosage), 0.25mg/mL (1x clinical dosage), 0.5mg/mL (2x clinical dosage), 1.0mg/mL (4x clinical dosage) risuteganib for dose-dependent assay, and incubated at 37°C for 1 hour before the start of the experiment. Measurements of oxygen consumption rate (OCR, measured by oxygen concentration change) and extracellular acidification rate (ECAR, measured by pH change) were taken. Changes in OCR and ECAR value were recorded prior to any perturbation, and then in response to sequential injections of treatments/inhibitors: oligomycin (ATP synthase inhibitor, MilliporeSigma), carbonyl cyanide 4-(trifluoromethoxy)phenylhydrazone (FCCP, mitochondrial respiration uncoupler, MilliporeSigma), and a mixture of antimycin and rotenone (electron transport blockers, MilliporeSigma). These agents were injected through ports of the Seahorse cartridges to reach final concentrations of 1, 0.5, and 1 μ M, respectively. After the assays, plates were saved, and protein readings were measured to normalize the cell number in each well.

3.3 Potential inhibition of pyruvate dehydrogenase kinase

On the way to search for RPE-mitochondria-OXPHS connections to risuteganib, we came across a nature product dichloroacetate (DCA). It shares some chemical similarities with the non-canonical amino acid, cysteic acid, as two chloride atoms in the chemical structure pull the electrons away from the carboxyl group (**Figure 3.4A**), making it more acidic, with pKa 1.35⁷⁴, while cysteic acid was reported to have a pKa value at 1.3⁷⁵.

DCA is a well-established inhibitor for pyruvate dehydrogenase kinase (PDK) (**Figure 3.4B**)⁷⁶. PDK is the molecular switch that deactivates the pyruvate dehydrogenase (PDH) by phosphorylation in mitochondria, which suppresses oxidative phosphorylation metabolism through tricarboxylic acid cycle (TCA)⁷⁷. PDK1, among the identified four isoforms, is specifically upregulated by HIF-1 in hypoxic conditions⁷⁸. Inactivation of PDK isoforms by the specific inhibitor DCA has beneficial effects in diabetes⁷⁹, lactic acidosis⁸⁰, myocardial ischemia⁸¹, and, potentially, cancer⁸². Limited research has been done to study DCA as a drug for retinal disease and RPE cells⁸³. Nevertheless, it has been suggested that PDK, the mitochondrial metabolic switch, represents a potential therapeutic target to protect against macular degeneration in the retina⁸⁴.

A



B

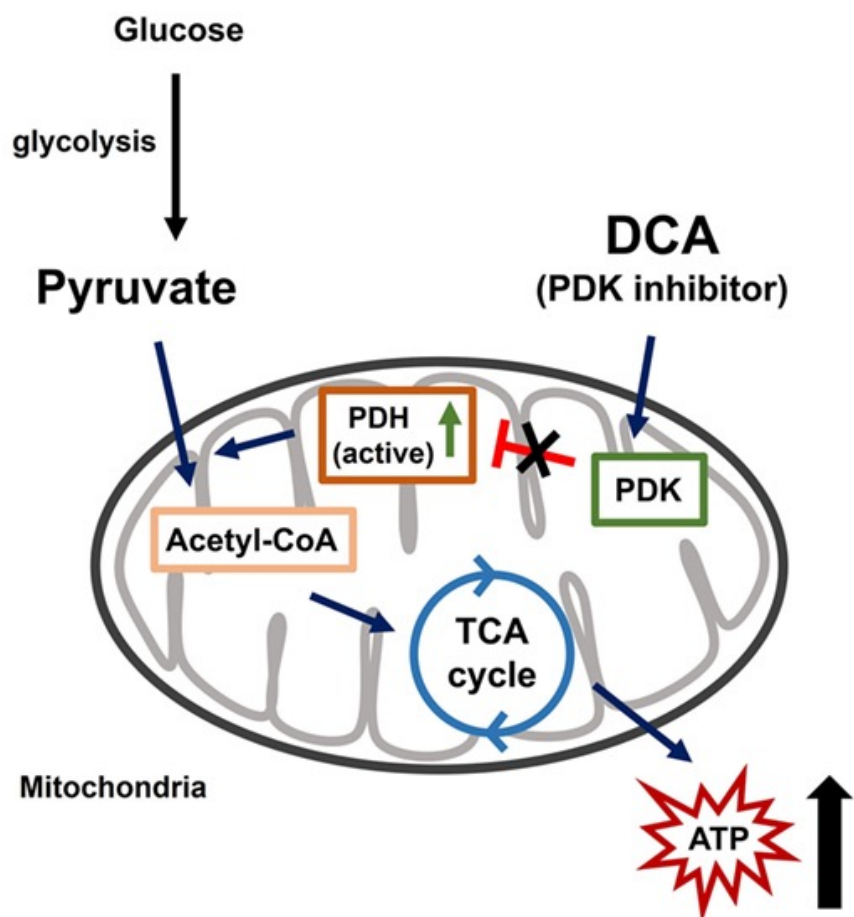


Figure 3.4 Dichloroacetic acid (DCA) is an inhibitor to pyruvate dehydrogenase kinase (PDK). (A) Risuteganib may share similar chemical properties with DCA. (B) Its function in the inhibition of PDK results in elevated oxidative phosphorylation with more ATP production. PDH: pyruvate dehydrogenase; Acetyl-coA: acetyl coenzyme A; TCA: tricarboxylic acid. Picture modified from literature⁸⁵.

3.3.1 Results

To test the hypothesis that risuteganib inhibits pyruvate dehydrogenase kinase (PDK), we measured the levels of phosphorylation on its substrate using recombinant proteins. PDK1, known to be inhibited by DCA at mM range, was incubated with its substrate, pyruvate dehydrogenase E1 subunit alpha 1 (PDHa1), with or without 2mM inhibitors (DCA, risuteganib, GRGETP). Immunoblotting was performed to detect total substrate and phosphorylated substrate after reaction. Total substrate, PDHa1, was detected using an antibody that bind all forms of PDHa1. Its phosphorylated version, PDHa1 phosphorylated at the serine residue at position 232 (PDHa1 pSer²³²), was detected by an antibody that specifically targets its phosphorylated counterpart.

Relatively low antibody-binding occurs in the absence of PDK1 (lane 1, **Figure 3.5**). The amount of phosphorylation when PDK1 is present (lane 2) is decreased by introducing 2mM DCA (lane 3). Introduction of 2mM risuteganib (lane 4) has a significantly greater inhibitory effect than DCA, while the control peptide GRGETP shows negligible inhibition of phosphorylation relative to PDK1 alone (lane 5).

We also need to keep in mind that pH may affect the structure and activity of PDK. A significant loss in the structure and activity can be observed under acidic conditions, specifically at pH less than 6⁸⁶. As DCA and risuteganib both have strong acid moiety (**Figure 3.4A**), we used assay buffer (25mM Tris or 25mM HEPES in universal kinase kit) that provides enough buffer capacity to maintain the pH between 7-8.

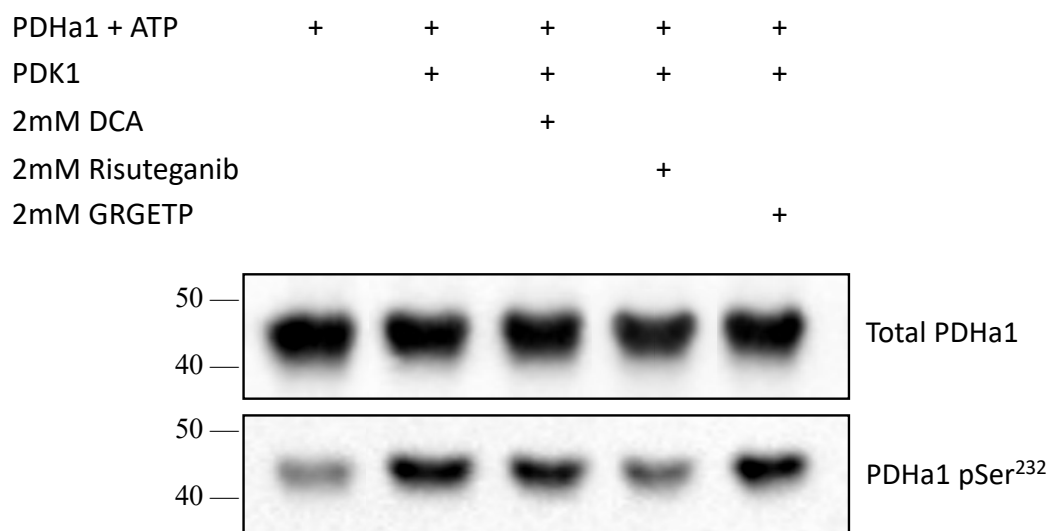


Figure 3.5 PDHa1 detection of phosphorylation at Ser²³² by immunoblotting. PDHa1 with ATP was left untreated (lane 1) or phosphorylated by incubating with PDK1 (lane 2-5). Known inhibitor dichloroacetate (DCA, lane 3) is compared to risuteganib (lane 4) or GRGETP Peptide (lane 5) by co-incubation with PDK1. Incubations lasted 30min at 37°C. Total PDHa1 and its counterpart phosphorylated at Ser²³² (PDHa1 pSer²³²) were western blotted by antibodies.

3.3.2 Discussion

We did not have much hope when we tested the possibility of PDK inhibition, as risuteganib's molecular structure is quite different from that of DCA. However, the protein kinase assay turned to be very interesting. The phosphorylation on PDH Ser²³² is greatly reduced by risuteganib, which indicates that risuteganib may be an inhibitor to PDK, even better than DCA. Based on the PDK inhibition by risuteganib, PDH activation may explain the observed elevated OXPHOS, as PDH is at the center of aerobic carbohydrate metabolism.

This study revealed that risuteganib may inhibit PDK, which induces more PDH in its active form. This provides a plausible explanation for the observed ATP production, which may explain improved mitochondrial integrity in RPE *in vitro*. Improved RPE function could explain the observed clinical benefits of risuteganib, which provided us with a novel view of the mechanism of action of risuteganib.

3.3.3 Methods

PDHa1 phosphorylation by PDK1

PDHa1 (MilliporeSigma) was phosphorylated by PDK1 (MilliporeSigma) using a universal kinase activity kit (R&D Systems). 30µg/mL PDHa1, 50µM ATP, 6µg/mL PDK1, and 2mM inhibitor, dichloroacetate (DCA, MilliporeSigma), and Risuteganib (CPC Scientific Peptide) or GRGETP Peptide (CPC Scientific Peptide) were used in this study. For each sample, enzyme, substrate, ATP, and inhibitors were freshly prepared in kinase buffer from the kit,

and mixed with PDK1 (added last, immediately prior to incubation), followed by a 30min incubation at 37°C.

Immunoblotting for PDHa1 phosphorylation

After 30min incubation at 37°C, the mixture was prepared for SDS-PAGE gel electrophoresis and transferred to western blot membrane, followed by overnight blocking in PBS with 5% BSA and 0.05% Tween20. The membrane was first immunostained by anti-pyruvate dehydrogenase rabbit mAb (Cell Signaling Technology) and secondary antibody anti-rabbit IgG HRP (Thermo Fisher Scientific) to reveal total PDHa1. Chemiluminescence reagent, Western Lightning Plus-ECL (Perkin Elmer) was used to provide detectable signals and imaged in Bio Rad imaging system ChemiDoc XRS+. The same membrane was then stripped with stripping buffer, 60mM Tris-HCl pH 6.8, 2% sodium dodecyl sulfate (SDS, MilliporeSigma) and 100mM 2-mercaptoethanol (BME, MilliporeSigma), and immunostained by anti-[phosphorylated pyruvate dehydrogenase pSer²³²] rabbit pAb (MilliporeSigma) and secondary antibody anti-rabbit IgG HRP to reveal the phosphorylated PDHa1 pSer²³², detected using the same chemiluminescent reagent and imaging method.

3.4 Enzymatic effect in RPE cell model

The protein kinase assay performed between PDK1 and PDHa1 shows that risuteganib may inhibit PDK1, resulting in less phosphorylation on the PDHa1, which may explain why oxidative phosphorylation and ATP-related respiration, not glycolysis, increased in a dose-dependent manner with risuteganib treatment in §3.2. However, there are four isoforms of PDK, and other pathways, including dephosphorylation of PDH by pyruvate dehydrogenase

phosphatase (PDP) and transcriptional controls, have great impact on PDH activity^{87,88}

(Figure 3.6). Would risuteganib's inhibition to PDK1 still have a strong enough effect on PDH activity in RPE cells? To answer this question, we check for the possibility that risuteganib inhibition effect on PDK may increase PDH activity *in vitro*, by examining PDH activity with or without risuteganib in an RPE cell model.

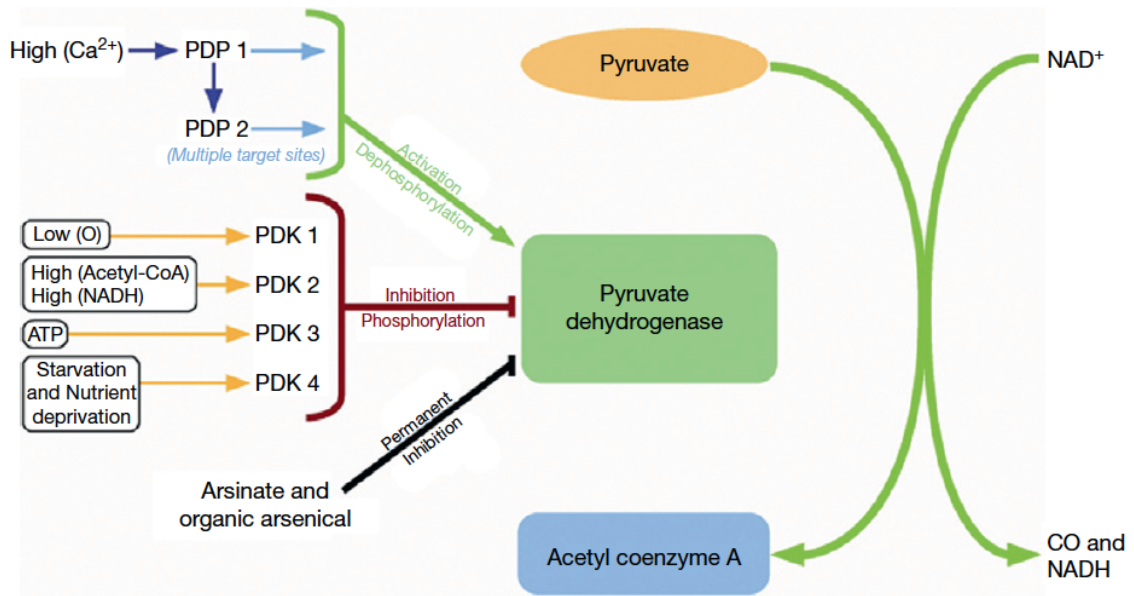


Figure 3.6 Pyruvate dehydrogenase (PDH) enzymatic functions and regulations. PDH catalyzes pyruvate to acetyl coenzyme A by converting NAD⁺ to NADH, and is regulated by pyruvate dehydrogenase kinase (PDK) and pyruvate dehydrogenase phosphatase (PDP)

3.4.1 Results

In vitro PDH enzymatic activity is examined in 30-day differentiated ARPE19 cells, with 24-hour preincubation with 300 μ M risuteganib or 300 μ M control peptide, GRGETP, in the cell culture medium prior to measurements. Both peptide cases were compared to untreated samples that receive medium without peptide added. Cells were then harvested, lysed, and centrifuged to collect supernatant with PDH enzyme in the buffer. PDH enzymatic activity was measured using a assay kit that provides a controlled concentration of pyruvate, and the production of nicotinamide adenine dinucleotide (NADH) was measured using coupled enzyme reaction with colorimetric readout at 450nm. The cells pretreated with risuteganib had significantly increased PDH enzyme activity by 14.0% ($p=0.0008$, $N=4$) relative to reference samples, while the control peptide RGE showed no difference relative to the reference group (**Figure 3.7**).

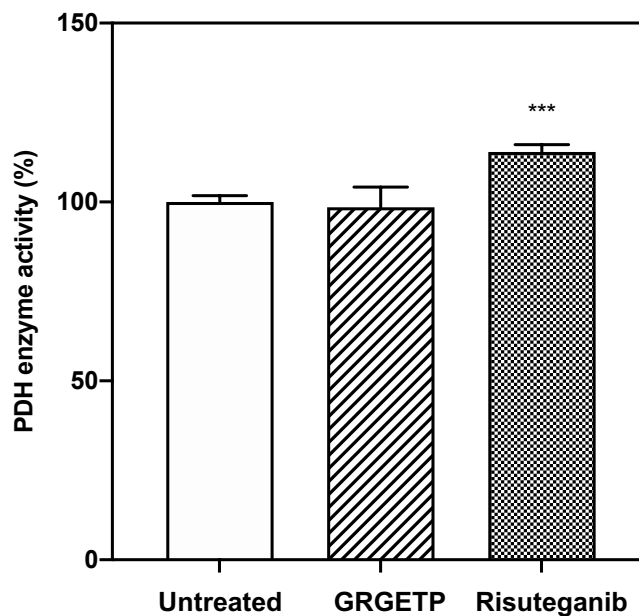


Figure 3.7 Risuteganib increases pyruvate dehydrogenase (PDH) enzyme activity in ARPE19 cells. ARPE19 cells treated with 300 μ M risuteganib or GRGETP control peptide were compared to cells that received fresh medium without peptide. Following 24hr incubation, PDH enzyme activity was measured by assay kit. Risuteganib treated cells showed significantly increased PDH activity than untreated cells (114.0% versus 100.0%, $p=0.0008$, $N=4$), whereas GRGETP peptide treatment had no measurable effect (98.5% versus 100%, $p=0.5737$, $N=4$). Data are mean \pm SD. *** $p<0.001$ versus corresponding untreated group.

3.4.2 Discussion

PDH enzyme, the gatekeeper of oxidative phosphorylation in mitochondria, was activated by risuteganib in the ARPE19 cell model. The results from the *in vitro* PDH enzymatic activity study provided an important piece of evidence to connect risuteganib's effects to mitochondrial function that is essential for cell survival. Inhibition of PDK by risuteganib results in increased PDH activity, which leads to an increase in the oxidative phosphorylation metabolism and allows more ATP turnover (§3.2). Mitochondrial bioenergetic regulation improves mitochondrial function, and protect mitochondria from oxidative stress, which result in the protective effect on cells under disease conditions (§2.5).

3.4.3 Methods

Pyruvate dehydrogenase (PDH) enzyme activity assay

Pyruvate dehydrogenase activity is determined by assay kit from MilliporeSigma, using a coupled enzyme reaction, which results in a colorimetric (450 nm) product. ARPE19 cells were grown on a transwell membrane and differentiated for 30 days to restore RPE phenotype, as described in Chapter 2. Cells were treated with 300µM risuteganib, 300µM GRGETP peptide, or no peptide as control in the culture medium for 24 hours at 37°C. After treatment, cells were washed with PBS twice, detached by accutase cell detachment solution (Innovative Cell Technologies), and collected by centrifugation. 1×10^6 cells were homogenized in 100µL ice-cold PDH assay buffer and kept on ice for 10 minutes. Insoluble materials were removed by 10,000 xg centrifugation. Protein concentration of each sample

was measured using Pierce BCA protein assay kit (Thermo Fisher Scientific). PDH assay buffer, developer, and substrate were mixed at 46:2:2 ratio to prepare the reaction mixture. Each sample was mixed 1:1 with the reaction mixture and the absorbance at 450nm was measured every 5min at 37°C. NADH standards were measured to generate a calibration curve. The PDH activity was calculated by the amount of NADH generated in the sample well divided by reaction time and sample volume. All the data were normalized to mean value observed in untreated group.

3.5 Current hypothesis on mechanism of action of risuteganib

In this journey to find the mechanism of action of risuteganib for treating retinal diseases, we have dived through several layers:

- 1) The peptide-directed fluorescent labeling study reveals that risuteganib preferentially binds with the retinal pigment epithelium (RPE) layer.
- 2) The *in vitro* study with an RPE cell model, ARPE19, shows that risuteganib significantly increases cell viability, reduces reactive oxygen species (ROS), and protects mitochondrial integrity.
- 3) The mitochondrial bioenergetics study with ARPE19 cells shows that risuteganib increases oxidative phosphorylation (OXPHOS) and ATP-related respiration, but has no effect on glycolysis.
- 4) Protein kinase assay and enzymatic activity assay reveal molecular interaction between risuteganib and a mitochondrial enzyme in OXPHOS. Risuteganib inhibits

pyruvate dehydrogenase kinase isoform 1 (PDK1) activity, which results in activated pyruvate dehydrogenase (PDH) activity.

Here, based on the experimental evidence we collected, we propose a hypothesis for potential mechanism of action for risuteganib drug effect that was observed clinically. In DR and AMD, activated HIF-1 α under disease conditions directly activates PDK1, which inactivates PDH in the OXPHOS metabolism in the mitochondria, resulting in imbalanced energy supply in RPE cells. The dysfunction of RPE mitochondria contributed to the early stage of disease development, including drusen formation and breakdown of blood-retinal barrier. Risuteganib, as a potential PDK1 inhibitor, turns the switch back to OXPHOS by activating PDH activity, allowing more ATP production to protect mitochondrial integrity and support RPE cell functions. RPE cells with enhanced bioenergetics could then keep the homeostasis of the retina tissue and protect the retina from disease conditions (**Figure 3.8**).

This new MOA may lead to a novel therapy orthogonal to anti-VEGF therapy. Anti-VEGF works efficiently in reducing neovascularization and draining accumulated fluid off the retina, which prevents the tissue structure being torn apart by angiogenesis. However, elevation in growth factors in the tissue is just the symptom of the diseases. When cells are under disease conditions, this triggers an inflammatory response to help solve the problem. Growth factors, like VEGF, are mediators to help facilitate this process, and restore tissue functions. Inhibition of angiogenesis may serve short-term benefits but has no effect or even adverse effect on the root cause. Cells without enough angiogenesis, lacking oxygen and nutrients, are at higher risk of degeneration, which was observed in some patients with long-

term anti-VEGF treatment. Risuteganib, with a potential drug efficacy through the proposed MOA, would restore the housekeeping cell layer, RPE, by elevating OXPHOS and ATP production, providing a possibility to treat the retinal diseases at the root cause.

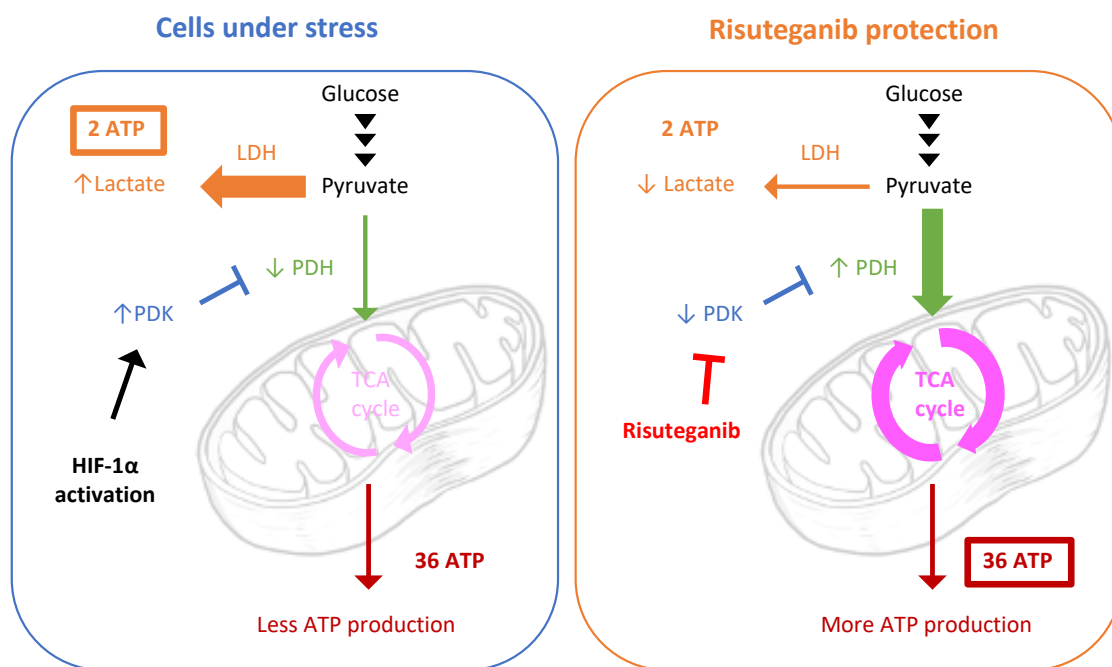


Figure 3.8 Proposed hypothesis of mechanism of action of risuteganib on regulating mitochondrial functions. LDH: lactate dehydrogenase; PDH: pyruvate dehydrogenase; PDK: pyruvate dehydrogenase kinase; HIF-1 α : hypoxia-induced factor 1 alpha; TCA: tricarboxylic acid.

Chapter IV

SUMMARY AND FUTURE WORK

4.1 Retracing our path along this journey

Looking back to the steps we took, I realized that our approach was unconventional for drug discovery. Most research was done in the order of identifying the protein of interest, designing the drug candidates that target the protein, and performing preclinical and clinical studies to evaluate the drug efficacy. For this study, we are really fortunate to study a peptide drug that has already shown promising clinical effects. We investigate where the drug effects come from by nailing down from tissue level, to cell level, to cellular organelle level, and finally to molecular level, which was really exciting each time we moved on from one level to the next.

It was a brave decision that we made not to be limited to the originally proposed MOA, as we found out that the experimental evidence did not support it. With unbiased peptide-directed fluorescent labeling, we were able to identify a cell layer that we have never thought it would bind to, the RPE layer. The connections between retinal diseases and malfunction of RPE mitochondria opened up a whole new direction of study, which led to our collaborations with Dr. Kenny at UC Irvine, Dr. Peter Campochiaro at Johns Hopkins University, Dr. Glenn Jaffe at Duke University, and Dr. Hugo Quiroz-Mercado at the University of Colorado. The most interesting part was to form a hypothesis on targeting the enzymatic regulation in mitochondrial metabolism and provide evidence to support the hypothesis by cellular and molecular studies. What has been uncovered in this study also has

great impact on how the biopharmaceutical company shifts their directions for this peptide drug in clinical trials. They are now aiming for treating retinal diseases in a much larger patient population, dry AMD to be more specific, which was not even relevant to the originally proposed MOA for targeting integrin and inhibiting angiogenesis.

It is interesting to note that there are a few other layers of the retina that are rich in mitochondria⁹⁰. Using an immunostaining for a mitochondria-specific biomarker, cytochrome c oxidase (COX IV), we confirmed prior literature regarding the distribution of mitochondria in the rat retina: the bands are seen at 1) RPE, 2) inner segment of the photoreceptor, and 3) inner plexiform layer (**Figure S4.1**). Consistent with my hypothesis that the binding partner is PDK, which is localized to mitochondria, the distribution of risuteganib-Cy5 binding shows a similar binding pattern to COX IV. In my suggestions for the future work, it would be recommended that the next step in colocalization experiments use immunostaining for PDK1 (more specific than COX IV) and use risuteganib-Cy5 (and GRGETP-Cy5 as control) to further examine co-localization.

4.2 Research and clinical observations agree with the current hypothesis

Although the new mitochondrial targeting mechanism is very different from the original MOA, we are surprised to find that it is consistent with a lot of research results that we had before. Moreover, we are able to explain several puzzles observed in research studies and clinical trials.

Dr. Zach Shao, a former graduate student in our group, studied gene regulations by risuteganib in a mouse model that mimics angiogenesis disease condition in the retina. Disease-related mouse model RNA-seq result showed oxidative phosphorylation pathways up-regulated by risuteganib at both RA and ROP conditions.

Dr. Hugo Quiroz-Mercado at the University of Colorado studied the risuteganib's protective effect on ganglion cells in rats with ischemic condition. The ischemia of the optical nerve was created by clamping the eyes for 60 minutes. A single dosage of risuteganib showed protective effect on the ganglion cells integrity and reduced cell apoptosis under hypoxia.

Among over 200 patients treated with risuteganib in Phase I and Phase II clinical trials, there is no drug toxicity reported that is directly related to the drug itself (adverse effects reported are all from the injections). It can be explained by that risuteganib only targets stressed cells with activated PDK. The PDK regulation may only affect oxidative phosphorylation but not glycolysis. As there are several metabolic pathways in the cells, regulating PDK would not leave cells with only one way to go, but would provide more energy compared to others.

In the clinical trials, the drug efficacy of visual acuity improvement and macular thickness reduction lasted for least three months after drug administration, much longer than typical small peptides. It can be explained by the drug effect from risuteganib that targets the mitochondrial metabolism, protects cells from stress conditions, and restores the normal RPE and photoreceptor function, which maintain the homeostasis of the whole retina tissue.

4.3 Broader context of inhibitors of pyruvate dehydrogenase kinase

The mitochondrial targeting strategy is not only for retinal diseases, but also broadly applicable to metabolic disorders, cardiovascular diseases, inflammatory diseases, neurodegenerative diseases, and cancer⁹¹. Evidence from preclinical studies, including asthma model and neurodegenerative model, and clinical trials, including retinitis pigmentosa, dry eye, and atopic dermatitis, indicates that risuteganib has broad applications on different diseases. Being able to uncover the mechanism of a safe and effective drug for more patients is a great pleasure and fulfillment for me.

What gets more interesting for me is seeing a possibility for risuteganib and its PDK targeting mechanism to treat cancers. Cancer cells rely heavily on glycolysis even in the presence of sufficient oxygen supply, known as the Warburg effect. The low efficiency of ATP production drives cancer cells to uptake much more glucose and other nutrients with altered proliferating cell profiles. PDK is reported to be activated in cancer cells as HIFa is stabilized in cancer cells. What if we could use PDK inhibitors that would alter cancer cell bioenergetics? With enough ATP provided in the mitochondria, it is possible to transform cancer cells into quiescent cells in the tissue.

This gets really personal to me. One of my close family members passed away because of liver cancer when I was really young. Not being able to help and support her was a great loss in my life. I have been following up with strategies for treating cancers for years and when I learnt that PDK inhibition would be a possible target for risuteganib, I think she is guiding me towards this direction to help other cancer patients.

4.4 Recommendation for future work

Although we covered the different levels of exploring the mechanism of action of risuteganib, there is still a lot more we need to work on to validate this hypothesis:

1. Matrix-assisted laser desorption/ionization (MALDI) mass spectrometry imaging may be performed to validate the binding loci, using non-labeled risuteganib in a disease-related animal model.
2. Immunostaining of the binding target, PDK1, along with peptide-directed fluorescent staining in cells or tissue may be performed to validate the colocalization between risuteganib and its binding partner.
3. Molecular binding assay using surface plasmon resonance (SPR) or enzyme-linked immunosorbent (ELISA) assays may be conducted to evaluate the binding constant.
4. Peptide-directed capture with a trifunctional molecule with (1) risuteganib on one end, (2) crosslinker on the second end, and (3) affinity tag on the third end, may be a good tool to study the binding site for risuteganib on PDK.

As mitochondria-targeting and PDK inhibition may provide therapeutic benefits to broader applications, it would be worth exploring some related research areas:

1. Structure-activity relationship (SAR) study may be performed to design risuteganib analogs for higher inhibition ability to PDK1 by (1) varying the location of sulfonic acid in the peptide, (2) varying the length of the peptide, (3) varying the distance

between sulfonic acid residue and the peptide backbone, and (4) varying strong acid on the residue.

2. Drug applications may be extended to metabolic disorders, cardiovascular diseases, inflammatory diseases, neurodegenerative diseases, and cancer with disease-related cell models or animal models.

Figure S2.1 Purification of risuteganib-Cy5 (A) and GRGETP-Cy5 (B) conjugates using prep-HPLC, and characterization with MALDI-TOF. The HPLC eluted fraction that contains the correct m/z value (m/z 1103 for risuteganib-Cy5, and m/z 1067 for GRGETP-Cy5) were collected (detailed methods in 2.2.2)

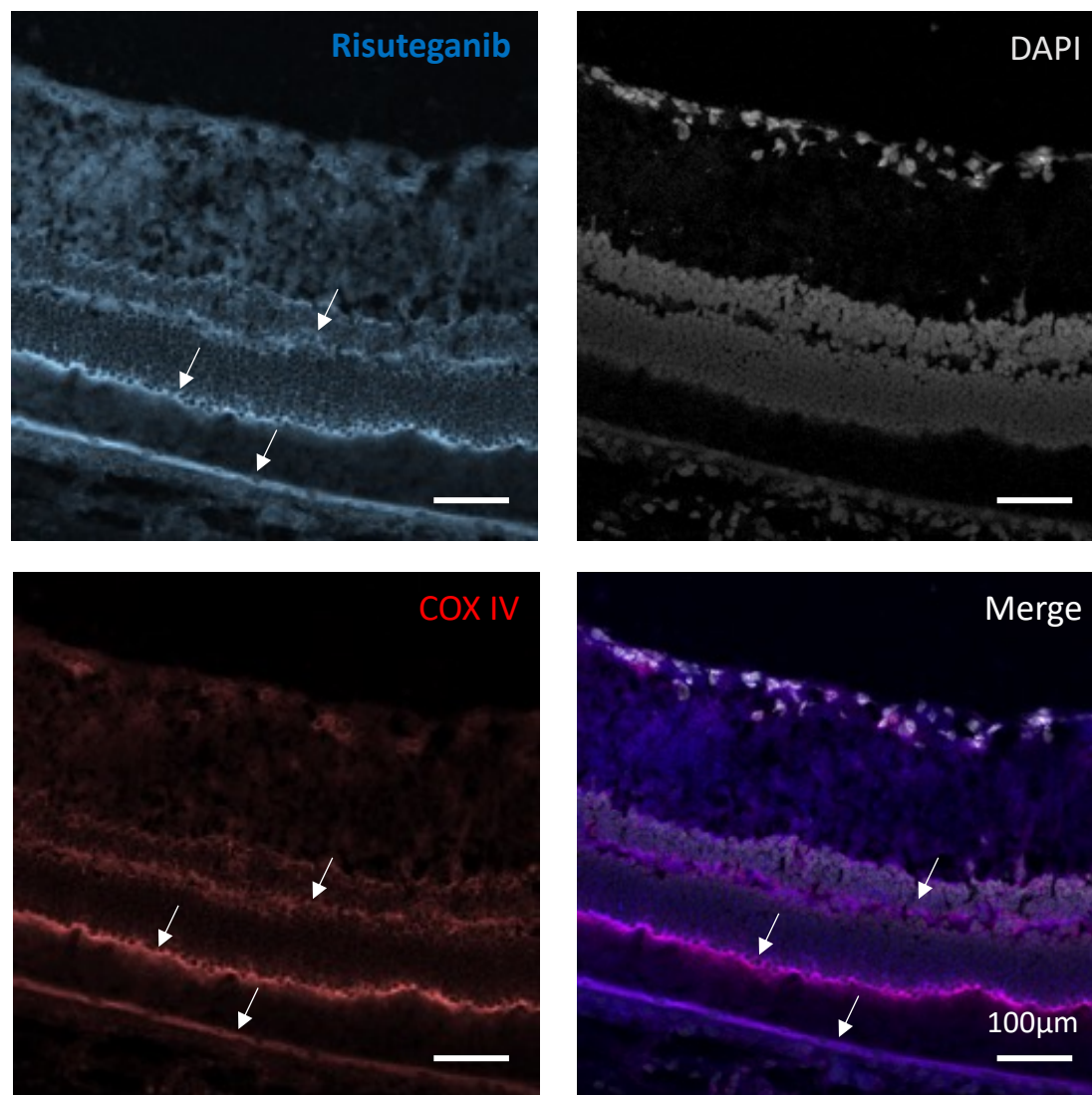


Figure S4.1 Colocalization of risuteganib and mitochondrial marker cytochrome c oxidase (COX IV) in rat retinal tissue. Anti-COX IV antibody stains mitochondria that are abundant in inner plexiform layer, inner segment of photoreceptor and RPE (white arrows). 1µM risuteganib-Cy5 colocalizes with mitochondria distribution in the retina, which showed purple color in the merge.

Methods for staining of rat retina with peptide-Cy5 and anti-COX IV antibody

Albino rats in this study were obtained from the Office of Laboratory Animal Resources (OLAR) at Caltech. Immediately after receiving the animal tissue, rat eyes were embedded in glycol-based optimal cutting temperature compound (OCT, Sakura Finetek USA) and flash frozen in liquid nitrogen. Frozen serial sections (10 μ m thick) were cut through the retinal region and mounted on glass slides. Sections were fixed by incubating in 4°C 4% paraformaldehyde for 10 minutes and washed with 10mM phosphate buffered saline (PBS, pH 7.4, ThermoFisher). Tissue sections were permeabilized with 0.1% Triton X-100 (MilliporeSigma) for 10 minutes, blocked with 5% Bovine Serum Albumin (BSA, MilliporeSigma) in PBS for 1 hour at room temperature or overnight at 4°C.

Mitochondrial biomarker, complex IV (COX IV, also called cytochrome c oxidase) was stained with mouse anti-COX IV antibody (Thermofisher) in PBS containing 1% BSA for 1 hour, followed by goat anti-IgG Alexa 594 (Thermofisher) in PBS containing 1% BSA for 1 hour. Colocalization staining of risuteagnib-Cy5 was examined with 1 μ M peptide-Cy5 conjugate in PBS containing 1% BSA for 1 hour at room temperature. The stained sections were washed with 0.5% tween-20 (MilliporeSigma) in PBS three times to remove unbounded labels. Mounting medium Fluoroshield with DAPI (MilliporeSigma) was added onto of each section prior to placing the coverslip on the sections. All images were acquired with a Zeiss LSM 710 confocal microscope.

REFERENCE

- (1) Bressler, N. M. Age-Related Macular Degeneration Is the Leading Cause of Blindness . . . *JAMA* **2004**, *291* (15), 1900–1901. <https://doi.org/10.1001/jama.291.15.1900>.
- (2) Colijn, J. M.; Buitendijk, G. H. S.; Prokofyeva, E.; Alves, D.; Cachulo, M. L.; Khawaja, A. P.; Cougnard-Gregoire, A.; Merle, B. M. J.; Korb, C.; Erke, M. G.; Bron, A.; Anastasopoulos, E.; Meester-Smoor, M. A.; Segato, T.; Piermarocchi, S.; de Jong, P. T. V. M.; Vingerling, J. R.; Topouzis, F.; Creuzot-Garcher, C.; Bertelsen, G.; Pfeiffer, N.; Fletcher, A. E.; Foster, P. J.; Silva, R.; Korobelnik, J.-F.; Delcourt, C.; Klaver, C. C. W. Prevalence of Age-Related Macular Degeneration in Europe. *Ophthalmology* **2017**, *124* (12), 1753–1763. <https://doi.org/10.1016/j.ophtha.2017.05.035>.
- (3) Wong, W. L.; Su, X.; Li, X.; Cheung, C. M. G.; Klein, R.; Cheng, C.-Y.; Wong, T. Y. Global Prevalence of Age-Related Macular Degeneration and Disease Burden Projection for 2020 and 2040: A Systematic Review and Meta-Analysis. *Lancet Glob Health* **2014**, *2* (2), e106-116. [https://doi.org/10.1016/S2214-109X\(13\)70145-1](https://doi.org/10.1016/S2214-109X(13)70145-1).
- (4) Zając-Pytrus, H.; Pilecka, A.; Turno-Kręcicka, A.; Adamiec-Mroczek, J.; Misiuk-Hojło, M. The Dry Form of Age-Related Macular Degeneration (AMD): The Current Concepts of Pathogenesis and Prospects for Treatment. *Adv Clin Exp Med* **2015**, *24* (6), 1099–1104. <https://doi.org/10.17219/acem/27093>.
- (5) Ng, E. W. M.; Adamis, A. P. Targeting Angiogenesis, the Underlying Disorder in Neovascular Age-Related Macular Degeneration. *Canadian Journal of Ophthalmology* **2005**, *40* (3), 352–368. [https://doi.org/10.1016/S0008-4182\(05\)80078-X](https://doi.org/10.1016/S0008-4182(05)80078-X).
- (6) Lim, L. S.; Mitchell, P.; Seddon, J. M.; Holz, F. G.; Wong, T. Y. Age-Related Macular Degeneration. *The Lancet* **2012**, *379* (9827), 1728–1738. [https://doi.org/10.1016/S0140-6736\(12\)60282-7](https://doi.org/10.1016/S0140-6736(12)60282-7).
- (7) Bhagat, N.; Grigorian, R. A.; Tutela, A.; Zarbin, M. A. Diabetic Macular Edema: Pathogenesis and Treatment. *Survey of Ophthalmology* **2009**, *54* (1), 1–32. <https://doi.org/10.1016/j.survophthal.2008.10.001>.
- (8) Retinopathy in Diabetes | Diabetes Care https://care.diabetesjournals.org/content/27/suppl_1/s84.short (accessed Apr 28, 2021).
- (9) Davson, H. *Physiology of the Eye*; Macmillan International Higher Education, 1990.

- (10) Provis, J. M.; Penfold, P. L.; Cornish, E. E.; Sandercoe, T. M.; Madigan, M. C. Anatomy and Development of the Macula: Specialisation and the Vulnerability to Macular Degeneration. *Clinical and Experimental Optometry* **2005**, *88* (5), 269–281. <https://doi.org/10.1111/j.1444-0938.2005.tb06711.x>.
- (11) Provis, J. M.; Hendrickson, A. E. The Foveal Avascular Region of Developing Human Retina. *Archives of Ophthalmology* **2008**, *126* (4), 507–511. <https://doi.org/10.1001/archopht.126.4.507>.
- (12) Provis, J. M.; Diaz, C. M.; Dreher, B. Ontogeny of the Primate Fovea: A Central Issue in Retinal Development. *Progress in Neurobiology* **1998**, *54* (5), 549–581. [https://doi.org/10.1016/S0301-0082\(97\)00079-8](https://doi.org/10.1016/S0301-0082(97)00079-8).
- (13) Joyal, J.-S.; Gantner, M. L.; Smith, L. E. H. Retinal Energy Demands Control Vascular Supply of the Retina in Development and Disease: The Role of Neuronal Lipid and Glucose Metabolism. *Prog Retin Eye Res* **2018**, *64*, 131–156. <https://doi.org/10.1016/j.preteyeres.2017.11.002>.
- (14) Kaur, C.; Foulds, W. S.; Ling, E. A. Blood–Retinal Barrier in Hypoxic Ischaemic Conditions: Basic Concepts, Clinical Features and Management. *Progress in Retinal and Eye Research* **2008**, *27* (6), 622–647. <https://doi.org/10.1016/j.preteyeres.2008.09.003>.
- (15) Al-Kharashi, A. S. Role of Oxidative Stress, Inflammation, Hypoxia and Angiogenesis in the Development of Diabetic Retinopathy. *Saudi Journal of Ophthalmology* **2018**, *32* (4), 318–323. <https://doi.org/10.1016/j.sjopt.2018.05.002>.
- (16) Neufeld, G.; Cohen, T.; Gengrinovitch, S.; Poltorak, Z. Vascular Endothelial Growth Factor (VEGF) and Its Receptors. *The FASEB Journal* **1999**, *13* (1), 9–22. <https://doi.org/10.1096/fasebj.13.1.9>.
- (17) Gupta, N.; Mansoor, S.; Sharma, A.; Sapkal, A.; Sheth, J.; Falatoonzadeh, P.; Kuppermann, B.; Kenney, M. Diabetic Retinopathy and VEGF. *Open Ophthalmol J* **2013**, *7*, 4–10. <https://doi.org/10.2174/1874364101307010004>.
- (18) Das, A.; McGuire, P. G. Retinal and Choroidal Angiogenesis: Pathophysiology and Strategies for Inhibition. *Progress in Retinal and Eye Research* **2003**, *22* (6), 721–748. <https://doi.org/10.1016/j.preteyeres.2003.08.001>.
- (19) Learn | Science Of AMD.
- (20) Rosenfeld, P. J.; Brown, D. M.; Heier, J. S.; Boyer, D. S.; Kaiser, P. K.; Chung, C. Y.; Kim, R. Y. Ranibizumab for Neovascular Age-Related Macular Degeneration. *New England Journal of Medicine* **2006**, *355* (14), 1419–1431. <https://doi.org/10.1056/NEJMoa054481>.

- (21) Spaide, R. F.; Laud, K.; Fine, H. F.; Klancnik, J. M. J.; Meyerle, C. B.; Yannuzzi, L. A.; Sorenson, J.; Slakter, J.; Fisher, Y. L.; Cooney, M. J. INTRAVITREAL BEVACIZUMAB TREATMENT OF CHOROIDAL NEOVASCULARIZATION SECONDARY TO AGE-RELATED MACULAR DEGENERATION. *RETINA* **2006**, *26* (4), 383–390. <https://doi.org/10.1097/01.iae.0000238561.99283.0e>.
- (22) Heier, J. S.; Brown, D. M.; Chong, V.; Korobelnik, J.-F.; Kaiser, P. K.; Nguyen, Q. D.; Kirchhof, B.; Ho, A.; Ogura, Y.; Yancopoulos, G. D.; Stahl, N.; Vitti, R.; Berliner, A. J.; Soo, Y.; Anderesi, M.; Groetzbach, G.; Sommerauer, B.; Sandbrink, R.; Simader, C.; Schmidt-Erfurth, U. Intravitreal Aflibercept (VEGF Trap-Eye) in Wet Age-Related Macular Degeneration. *Ophthalmology* **2012**, *119* (12), 2537–2548. <https://doi.org/10.1016/j.ophtha.2012.09.006>.
- (23) Dugel, P. U.; Koh, A.; Ogura, Y.; Jaffe, G. J.; Schmidt-Erfurth, U.; Brown, D. M.; Gomes, A. V.; Warburton, J.; Weichselberger, A.; Holz, F. G. HAWK and HARRIER: Phase 3, Multicenter, Randomized, Double-Masked Trials of Brolucizumab for Neovascular Age-Related Macular Degeneration. *Ophthalmology* **2020**, *127* (1), 72–84. <https://doi.org/10.1016/j.ophtha.2019.04.017>.
- (24) Osaadon, P.; Fagan, X. J.; Lifshitz, T.; Levy, J. A Review of Anti-VEGF Agents for Proliferative Diabetic Retinopathy. *Eye (Lond)* **2014**, *28* (5), 510–520. <https://doi.org/10.1038/eye.2014.13>.
- (25) Rosenfeld, P. J.; Shapiro, H.; Tuomi, L.; Webster, M.; Elledge, J.; Blodi, B. Characteristics of Patients Losing Vision after 2 Years of Monthly Dosing in the Phase III Ranibizumab Clinical Trials. *Ophthalmology* **2011**, *118* (3), 523–530. <https://doi.org/10.1016/j.ophtha.2010.07.011>.
- (26) Home <https://www.allegroeye.com/> (accessed Apr 24, 2021).
- (27) Quiroz-Mercado, H. Integrin Peptide Therapy in Choroidal and Retinal Neovascularization. 2.
- (28) Kuppermann, B. D. A Dual-Mechanism Drug for Vitreoretinal Diseases. 3.
- (29) Friedlander, M.; Theesfeld, C. L.; Sugita, M.; Fruttiger, M.; Thomas, M. A.; Chang, S.; Cheres, D. A. Involvement of Integrins Alpha v Beta 3 and Alpha v Beta 5 in Ocular Neovascular Diseases. *PNAS* **1996**, *93* (18), 9764–9769. <https://doi.org/10.1073/pnas.93.18.9764>.
- (30) Maier, A.-K. B.; Kociok, N.; Zahn, G.; Vossmeier, D.; Stragies, R.; Muether, P. S.; Joussen, A. M. Modulation of Hypoxia-Induced Neovascularization by JSM6427, an Integrin A5β 1 Inhibiting Molecule. *Current Eye Research* **2007**, *32* (9), 801–812. <https://doi.org/10.1080/02713680701553052>.

- (31) Bhatwadekar, A. D.; Kansara, V.; Luo, Q.; Ciulla, T. Anti-Integrin Therapy for Retinovascular Diseases. *Expert Opin Investig Drugs* **2020**, *29* (9), 935–945. <https://doi.org/10.1080/13543784.2020.1795639>.
- (32) Ruoslahti, E. Fibronectin and Its Receptors. *Annu. Rev. Biochem.* **1988**, *57* (1), 375–413. <https://doi.org/10.1146/annurev.bi.57.070188.002111>.
- (33) Felding-Habermann, B.; Cheresch, D. A. Vitronectin and Its Receptors. *Current Opinion in Cell Biology* **1993**, *5* (5), 864–868. [https://doi.org/10.1016/0955-0674\(93\)90036-P](https://doi.org/10.1016/0955-0674(93)90036-P).
- (34) Mark, K. von der; Kühn, U. Laminin and Its Receptor. *Biochimica et Biophysica Acta (BBA) - Reviews on Cancer* **1985**, *823* (2), 147–160. [https://doi.org/10.1016/0304-419X\(85\)90010-1](https://doi.org/10.1016/0304-419X(85)90010-1).
- (35) Quiroz-Mercado, H.; Boyer, D. S.; Campochiaro, P. A.; Heier, J. S.; Kaiser, P. K.; Kornfield, J.; Kuppermann, B. D.; Karageozian, V. H.; Karageozian, H. L.; Karageozian, L.; Park, J. Y.; Sarayba, M. Randomized, Prospective, Double-Masked, Controlled Phase 2b Trial to Evaluate the Safety & Efficacy of ALG-1001 (Luminate®) in Diabetic Macular Edema. *Invest. Ophthalmol. Vis. Sci.* **2018**, *59* (9), 1960–1960.
- (36) Dugel, P.; Ma, S.; Ds, K. Multi-Factorial “Switch” Will Determine Efficacy of the Treatment. **2018**, 15.
- (37) Retinal Physician - Risuteganib for Intermediate Dry AMD <https://www.retinalphysician.com/issues/2019/november-2019/risuteganib-for-intermediate-dry-amd> (accessed Apr 24, 2021).
- (38) Green, R. J.; Davies, M. C.; Roberts, C. J.; Tendler, S. J. B. Competitive Protein Adsorption as Observed by Surface Plasmon Resonance. *Biomaterials* **1999**, *20* (4), 385–391. [https://doi.org/10.1016/S0142-9612\(98\)00201-4](https://doi.org/10.1016/S0142-9612(98)00201-4).
- (39) Giancotti, F. G.; Ruoslahti, E. Integrin Signaling. *Science* **1999**, *285* (5430), 1028–1033. <https://doi.org/10.1126/science.285.5430.1028>.
- (40) Galloway, N. R.; Amoaku, W. M. K.; Galloway, P. H.; Browning, A. C. Basic Anatomy and Physiology of the Eye. In *Common Eye Diseases and their Management*; Galloway, N. R., Amoaku, W. M. K., Galloway, P. H., Browning, A. C., Eds.; Springer International Publishing: Cham, 2016; pp 7–16. https://doi.org/10.1007/978-3-319-32869-0_2.
- (41) Modesti, M. Fluorescent Labeling of Proteins. In *Single Molecule Analysis: Methods and Protocols*; Peterman, E. J. G., Wuite, G. J. L., Eds.; Methods in Molecular Biology; Humana Press: Totowa, NJ, 2011; pp 101–120. https://doi.org/10.1007/978-1-61779-282-3_6.

- (42) Gonçalves, M. S. T. Fluorescent Labeling of Biomolecules with Organic Probes. *Chem. Rev.* **2009**, *109* (1), 190–212. <https://doi.org/10.1021/cr0783840>.
- (43) Simple Anatomy of the Retina by Helga Kolb – Webvision.
- (44) Berne & Levy Physiology - 7th Edition <https://www.elsevier.com/books/berne-and-levy-physiology/koeppen/978-0-323-39394-2> (accessed Apr 30, 2021).
- (45) Strauss, O. The Retinal Pigment Epithelium in Visual Function. *Physiol Rev* **2005**, *85* (3), 845–881. <https://doi.org/10.1152/physrev.00021.2004>.
- (46) Campbell, M.; Humphries, P. The Blood-Retina Barrier. In *Biology and Regulation of Blood-Tissue Barriers*; Cheng, C. Y., Ed.; Advances in Experimental Medicine and Biology; Springer: New York, NY, 2013; pp 70–84. https://doi.org/10.1007/978-1-4614-4711-5_3.
- (47) Zhang, X.; Zeng, H.; Bao, S.; Wang, N.; Gillies, M. C. Diabetic Macular Edema: New Concepts in Patho-Physiology and Treatment. *Cell & Bioscience* **2014**, *4* (1), 27. <https://doi.org/10.1186/2045-3701-4-27>.
- (48) Golestaneh, N.; Chu, Y.; Xiao, Y.-Y.; Stoleru, G. L.; Theos, A. C. Dysfunctional Autophagy in RPE, a Contributing Factor in Age-Related Macular Degeneration. *Cell Death & Disease* **2018**, *8* (1), e2537–e2537. <https://doi.org/10.1038/cddis.2016.453>.
- (49) Mannagh, J.; Arya, D. V.; Irvine, A. R. Tissue Culture of Human Retinal Pigment Epithelium. *Invest. Ophthalmol. Vis. Sci.* **1973**, *12* (1), 52–64.
- (50) Tso, M. O. M.; Albert, D.; Zimmerman, L. E. Organ Culture of Human Retinal Pigment Epithelium and Choroid: A Model for the Study of Cytologic Behavior of RPE in Vitro. *Invest. Ophthalmol. Vis. Sci.* **1973**, *12* (8), 554–566.
- (51) Fronk, A. H.; Vargis, E. Methods for Culturing Retinal Pigment Epithelial Cells: A Review of Current Protocols and Future Recommendations. *J Tissue Eng* **2016**, *7*, 204173141665083. <https://doi.org/10.1177/2041731416650838>.
- (52) Dunn, K. C.; Aotaki-Keen, A. E.; Putkey, F. R.; Hjelmeland, L. M. ARPE-19, A Human Retinal Pigment Epithelial Cell Line with Differentiated Properties. *Experimental Eye Research* **1996**, *62* (2), 155–170. <https://doi.org/10.1006/exer.1996.0020>.
- (53) Ahmado, A.; Carr, A.-J.; Vugler, A. A.; Semo, M.; Gias, C.; Lawrence, J. M.; Chen, L. L.; Chen, F. K.; Turowski, P.; da Cruz, L.; Coffey, P. J. Induction of Differentiation by Pyruvate and DMEM in the Human Retinal Pigment Epithelium Cell Line ARPE-19. *Invest. Ophthalmol. Vis. Sci.* **2011**, *52* (10), 7148. <https://doi.org/10.1167/iovs.10-6374>.

- (54) Samuel, W.; Jaworski, C.; Postnikova, O. A.; Kutty, R. K.; Duncan, T.; Tan, L. X.; Poliakov, E.; Lakkaraju, A.; Redmond, T. M. Appropriately Differentiated ARPE-19 Cells Regain Phenotype And. *Molecular Vision* **2017**, *30*.
- (55) Shao, Z. Biological Responses to Therapeutic Treatments of Human Vascular Diseases. 449.
- (56) Kowluru, R. A.; Chan, P.-S. Oxidative Stress and Diabetic Retinopathy. *Exp Diabetes Res* **2007**, *2007*. <https://doi.org/10.1155/2007/43603>.
- (57) Zarbin, M. A. Current Concepts in the Pathogenesis of Age-Related Macular Degeneration. *Archives of Ophthalmology* **2004**, *122* (4), 598–614. <https://doi.org/10.1001/archophth.122.4.598>.
- (58) Cai, J.; Nelson, K. C.; Wu, M.; Sternberg, P.; Jones, D. P. Oxidative Damage and Protection of the RPE. *Progress in Retinal and Eye Research* **2000**, *19* (2), 205–221. [https://doi.org/10.1016/S1350-9462\(99\)00009-9](https://doi.org/10.1016/S1350-9462(99)00009-9).
- (59) Sparrow, J. R.; Hicks, D.; Hamel, C. P. The Retinal Pigment Epithelium in Health and Disease. *Curr Mol Med* **2010**, *10* (9), 802–823. <https://doi.org/10.2174/156652410793937813>.
- (60) Sreekumar, P. G.; Ishikawa, K.; Spee, C.; Mehta, H. H.; Wan, J.; Yen, K.; Cohen, P.; Kannan, R.; Hinton, D. R. The Mitochondrial-Derived Peptide Humanin Protects RPE Cells From Oxidative Stress, Senescence, and Mitochondrial Dysfunction. *Invest. Ophthalmol. Vis. Sci.* **2016**, *57* (3), 1238. <https://doi.org/10.1167/iovs.15-17053>.
- (61) Brand, M. D. The Sites and Topology of Mitochondrial Superoxide Production. *Exp Gerontol* **2010**, *45* (7–8), 466–472. <https://doi.org/10.1016/j.exger.2010.01.003>.
- (62) Quinlan, C. L.; Goncalves, R. L. S.; Hey-Mogensen, M.; Yadava, N.; Bunik, V. I.; Brand, M. D. The 2-Oxoacid Dehydrogenase Complexes in Mitochondria Can Produce Superoxide/Hydrogen Peroxide at Much Higher Rates than Complex I. *J Biol Chem* **2014**, *289* (12), 8312–8325. <https://doi.org/10.1074/jbc.M113.545301>.
- (63) He, Y.; Ge, J.; Burke, J. M.; Myers, R. L.; Dong, Z. Z.; Tombran-Tink, J. Mitochondria Impairment Correlates with Increased Sensitivity of Aging RPE Cells to Oxidative Stress. *J ocul biol dis inform* **2010**, *3* (3), 92–108. <https://doi.org/10.1007/s12177-011-9061-y>.
- (64) Country, M. W. Retinal Metabolism: A Comparative Look at Energetics in the Retina. *Brain Research* **2017**, *1672*, 50–57. <https://doi.org/10.1016/j.brainres.2017.07.025>.
- (65) Age-Related Macular Degeneration | NEJM
https://www.nejm.org/doi/full/10.1056/NEJMra0801537?casa_token=NU2BNQMK

woYAAAAA%3ASsMQo51Phfuy1Ut-sbVgHNvhc9uTcw1ngC-nvwMMR_Ko2QaqI54HYAIPU9S3aAuCyAipjWWXk6Fj (accessed Apr 20, 2021).

- (66) Schmidt, K.-G.; Bergert, H.; Funk, R. H. W. Neurodegenerative Diseases of the Retina and Potential for Protection and Recovery. *Current Neuropharmacology* **2008**, *6* (2), 164–178. <https://doi.org/10.2174/157015908784533851>.
- (67) Dowling, J. E. *The Retina: An Approachable Part of the Brain*; Harvard University Press, 1987.
- (68) Kolb, H. How the Retina Works: Much of the Construction of an Image Takes Place in the Retina Itself through the Use of Specialized Neural Circuits. *American Scientist* **2003**, *91* (1), 28–35.
- (69) Lefevre, E.; Toft-Kehler, A. K.; Vohra, R.; Kolko, M.; Moons, L.; Van Hove, I. Mitochondrial Dysfunction Underlying Outer Retinal Diseases. *Mitochondrion* **2017**, *36*, 66–76. <https://doi.org/10.1016/j.mito.2017.03.006>.
- (70) Mitochondrial Decay and Impairment of Antioxidant Defenses in Aging RPE Cells | SpringerLink https://link.springer.com/chapter/10.1007/978-1-4419-1399-9_20 (accessed Apr 20, 2021).
- (71) Investigating Mitochondria as a Target for Treating Age-Related Macular Degeneration | Journal of Neuroscience <https://www.jneurosci.org/content/35/18/7304.short> (accessed Apr 20, 2021).
- (72) Voet, D.; Voet, J. G.; Pratt, C. W. *Fundamentals of Biochemistry: Life at the Molecular Level*; John Wiley & Sons, 2016.
- (73) Yetkin-Arik, B.; Vogels, I. M. C.; Nowak-Sliwinska, P.; Weiss, A.; Houtkooper, R. H.; Van Noorden, C. J. F.; Klaassen, I.; Schlingemann, R. O. The Role of Glycolysis and Mitochondrial Respiration in the Formation and Functioning of Endothelial Tip Cells during Angiogenesis. *Scientific Reports* **2019**, *9* (1), 12608. <https://doi.org/10.1038/s41598-019-48676-2>.
- (74) Haynes, W. M. *CRC Handbook of Chemistry and Physics*; CRC Press, 2014.
- (75) Dissociation Constants Of Organic Acids And Bases <https://www.zirchrom.com/organic.htm> (accessed Apr 26, 2021).
- (76) Whitehouse, S.; Cooper, R. H.; Randle, P. J. Mechanism of Activation of Pyruvate Dehydrogenase by Dichloroacetate and Other Halogenated Carboxylic Acids. *Biochem J* **1974**, *141* (3), 761–774. <https://doi.org/10.1042/bj1410761>.

- (77) Kato, M.; Li, J.; Chuang, J. L.; Chuang, D. T. Distinct Structural Mechanisms for Inhibition of Pyruvate Dehydrogenase Kinase Isoforms by AZD7545, Dichloroacetate, and Radicicol. **2010**, 24.
- (78) Kim, J.; Tchernyshyov, I.; Semenza, G. L.; Dang, C. V. HIF-1-Mediated Expression of Pyruvate Dehydrogenase Kinase: A Metabolic Switch Required for Cellular Adaptation to Hypoxia. *Cell Metab* **2006**, 3 (3), 177–185. <https://doi.org/10.1016/j.cmet.2006.02.002>.
- (79) Stacpoole, P. W. The Pharmacology of Dichloroacetate. *Metabolism* **1989**, 38 (11), 1124–1144. [https://doi.org/10.1016/0026-0495\(89\)90051-6](https://doi.org/10.1016/0026-0495(89)90051-6).
- (80) Henderson, G. N.; Curry, S. H.; Derendorf, H.; Wright, E. C.; Stacpoole, P. W. Pharmacokinetics of Dichloroacetate in Adult Patients with Lactic Acidosis. *J Clin Pharmacol* **1997**, 37 (5), 416–425. <https://doi.org/10.1002/j.1552-4604.1997.tb04319.x>.
- (81) Bersin, R. M.; Stacpoole, P. W. Dichloroacetate as Metabolic Therapy for Myocardial Ischemia and Failure. *Am Heart J* **1997**, 134 (5 Pt 1), 841–855. [https://doi.org/10.1016/s0002-8703\(97\)80007-5](https://doi.org/10.1016/s0002-8703(97)80007-5).
- (82) Michelakis, E. D.; Webster, L.; Mackey, J. R. Dichloroacetate (DCA) as a Potential Metabolic-Targeting Therapy for Cancer. *British Journal of Cancer* **2008**, 99 (7), 989–994. <https://doi.org/10.1038/sj.bjc.6604554>.
- (83) Shukal, D.; Bhadresha, K.; Shastri, B.; Mehta, D.; Vasavada, A.; Johar SR, K. Dichloroacetate Prevents TGF β -Induced Epithelial-Mesenchymal Transition of Retinal Pigment Epithelial Cells. *Experimental Eye Research* **2020**, 197, 108072. <https://doi.org/10.1016/j.exer.2020.108072>.
- (84) Lambert, V.; Hansen, S.; Schoumacher, M.; Lecomte, J.; Leenders, J.; Hubert, P.; Herfs, M.; Blacher, S.; Carnet, O.; Yip, C.; Blaise, P.; Duchateau, E.; Locht, B.; Thys, M.; Cavalier, E.; Gothot, A.; Govaerts, B.; Rakic, J.-M.; Noel, A.; de Tullio, P. Pyruvate Dehydrogenase Kinase/Lactate Axis: A Therapeutic Target for Neovascular Age-Related Macular Degeneration Identified by Metabolomics. *J Mol Med* **2020**, 98 (12), 1737–1751. <https://doi.org/10.1007/s00109-020-01994-9>.
- (85) Hong, D. K.; Kho, A. R.; Choi, B. Y.; Lee, S. H.; Jeong, J. H.; Lee, S. H.; Park, K.-H.; Park, J.-B.; Suh, S. W. Combined Treatment With Dichloroacetic Acid and Pyruvate Reduces Hippocampal Neuronal Death After Transient Cerebral Ischemia. *Front. Neurol.* **2018**, 9. <https://doi.org/10.3389/fneur.2018.00137>.
- (86) Anwar, S.; Kar, R. K.; Haque, Md. A.; Dahiya, R.; Gupta, P.; Islam, A.; Ahmad, F.; Hassan, Md. I. Effect of PH on the Structure and Function of Pyruvate Dehydrogenase Kinase 3: Combined Spectroscopic and MD Simulation Studies. *International Journal*

of *Biological Macromolecules* **2020**, *147*, 768–777.
<https://doi.org/10.1016/j.ijbiomac.2020.01.218>.

- (87) Patel, M. S.; Korotchkina, L. G. Regulation of the Pyruvate Dehydrogenase Complex. *Biochemical Society Transactions* **2006**, *34* (2), 217–222.
<https://doi.org/10.1042/BST0340217>.
- (88) Norton, L.; DeFronzo, R. Skeletal Muscle Glucose Metabolism and Insulin Resistance. In *Pathobiology of Human Disease*; Elsevier, 2014; pp 477–487.
<https://doi.org/10.1016/B978-0-12-386456-7.02003-7>.
- (89) Norton, L.; DeFronzo, R. Skeletal Muscle Glucose Metabolism and Insulin Resistance. In *Pathobiology of Human Disease*; McManus, L. M., Mitchell, R. N., Eds.; Academic Press: San Diego, 2014; pp 477–487. <https://doi.org/10.1016/B978-0-12-386456-7.02003-7>.
- (90) Chidlow, G.; Wood, J. P. M.; Sia, P. I.; Casson, R. J. Distribution and Activity of Mitochondrial Proteins in Vascular and Avascular Retinas: Implications for Retinal Metabolism. *Invest. Ophthalmol. Vis. Sci.* **2019**, *60* (1), 331.
<https://doi.org/10.1167/iovs.18-25536>.
- (91) Armstrong, J. S. Mitochondrial Medicine: Pharmacological Targeting of Mitochondria in Disease. *British Journal of Pharmacology* **2007**, *151* (8), 1154–1165.
<https://doi.org/10.1038/sj.bjp.0707288>.